Journal of Scientific Exploration, Vol. 18, No. 3, pp. 439–481, 2004 0892-3310/04

Ball Lightning and Atmospheric Light Phenomena: A Common Origin?

TORE WESSEL-BERG

Institute of Physical Electronics, Norwegian University of Science and Technology, N-7034 Trondheim, Norway
e-mail: tore.wessel-berg@fysel.ntnu.no

Abstract—The paper proposes a common origin of atmospheric light phenomena, including ball lightning and higher atmospheric lightnings such as UFOs and light emissions of various shapes. The emission of light from seemingly localized objects is described as the end stage of an electromagnetic process involving conversion of electric energy from the original distributed form between clouds to a concentrated form in a free space spherical circuit. The paper describes the localized fields as a standing wave of radial *D*irect *C*urrent (*DC*) pulses in a floating electrodeless ''free space circuit'' characterized by a strong field region at the center giving rise to ionization of gas molecules and light emissions. The presentation describes a sequence of events initiated by some atmospheric discharge such as a lightning bolt, followed by a parametric conversion process of the prestrike electric energy stored in the charged clouds, via magnetic energy during the strike, to poststrike electric energy stored in the spherical system. Because the electromagnetic field solutions specifying the particular spherical system have the form of transmission line equations, describing the fields as superpositions of traveling spherical waves, much of the theory is formulated on concepts drawn from regular transmission lines. The theory predicts formation of ball lightning objects near ground or higher altitude lightning objects of various shapes, emphasizing their common origin. The paper explains the motion of the localized ionized objects as due to interaction with the environmental electric fields of charged cloud systems, with no apparent limits on speed and acceleration including abrupt directional changes. The paper discusses the predicted characteristics of the lightning phenomena, in particular describing expected motions under specific circumstances, and showing these to be compatible with the bulk of observations, with no obvious contradictions.

Keywords: ball lightning—atmospheric light phenomena—transmission line—ionization

1. Introduction

Ball lightning occurs as a sporadic natural phenomenon during regular thunderstorms, but also under less extreme conditions of atmospheric disturbances (Stenhoff, 1999). From numerous sightings and reports by eyewitnesses, ball lightning is typically seen as the sudden appearance of a localized ball-shaped sphere of lightning, with size 0.2–1 meters, moving in a

non-systematic and unpredictable fashion. They are usually observed within close range of the ground, moving horizontally with random but moderate speeds of a few meters per second, typically lasting less than a minute, then decaying silently or by a noisy explosion.

There exists an abundance of reports and publications on ball lightning observations and proposed explanations, linking the phenomenon to a variety of physical and chemical processes, but none of these theories seem to have gained general acceptance because they fail to explain *all* the observed characteristics of the phenomenon. This is clearly reflected in the title of the recent book (Stenhoff, 1999), containing an up to date coverage and summary of sightings and a review of theories: *Ball Lightning—An Unsolved Problem in Atmospheric Physics*.

In a recent publication the author (Wessel-Berg, 2003) proposed an explanation of ball lightning as a simple electromagnetic phenomenon triggered by atmospheric discharges such as lightning bolts. The purpose of the present paper is to expand the same basic theory to encompass a wider group of observed light phenomena in the sky, which differ from ball lightning but appear to share some common characteristics such as sudden appearance and disappearance of luminous object-like structures at some height above ground. The most notable sightings of these kinds are those classified as ''Unidentified Flying Objects'' (UFO), which perhaps more than any other natural phenomenon have triggered speculations of their origin and true nature (Sturrock, 1999). There are also reports of local regular sightings of atmospheric light phenomena of various shapes such as the ones observed in Hessdalen, Norway (Sturrock, 1999: 78–80), which appear to be different from typical UFO sightings. However, certain common features exhibited by most events involving luminous sky phenomena, including ball lightning, seem to suggest a common physical origin for all.

The association of luminous sky phenomena to electromagnetic origins is certainly not new. In particular this is true for ball lightning with many theories suggested by a number of workers (Endean, 1976; Kapitza, 1958). These share the common feature of being some kind of high frequency resonance excited during thunder strikes. The absence of success for these theories in explaining all observable aspects of ball lightning suggests that either some new physics is needed, or that the basic physics is known but not recognized due to some hidden assumption in treating the problem. In the proposed explanation the author takes the view that no new physics is needed, linking ball lightning to simpler but perhaps unfamiliar electromagnetic phenomena. These involve certain localized and stationary *DC* field solutions of a free space spherical transmission line and their excitation by atmospheric current discharges via a conversion process related to *parametric* phenomena in electromagnetic theory. In the present paper these ideas are generalized to possibly embrace the wider class of luminous light phenomena. The emphasis of the purely explorative investigation is to demonstrate a possible common ground, with

no claims made about full coverage and complete understanding of all aspects of the sightings.

The paper links the occurrence of atmospheric light phenomena to a special electromagnetic process taking place during an atmospheric discharge of accumulated charges between cloud formations or from clouds to ground. Although the overall discharge mechanism appears to be fairly complex, the dominating feature is an energy conversion process related to *parametric* phenomena in electromagnetic theory. The phenomenon is of parametric type because of the conducting channel being switched on and off during the discharge, thereby affecting an abrupt time-varying change in one of the electromagnetic parameters (the channel conductivity). The theory describes how the major part of the stored *DC* electric energy before the strike is first converted to magnetic energy upheld by the channel current, and subsequently transferred back to electric energy stored as a *DC* standing wave in an electrodeless spherical transmission line system in free space. In this spherical system the electric field strength is proportional to $1/r$ and is therefore expected to cause ionization of the surrounding air inside a spherical boundary around $r = 0$. Although the theory associates ball lightning with the ideal spherical system, it is shown that various environmental perturbations might give rise to deviations from the spherical form, possibly explaining other kinds of atmospheric sightings beside ball lightning.

The first part of the paper presents the basic theory of the electromagnetic solutions for the spherical transmission line, the basis of the parametric excitation, and the ionization process claimed to cause ball lightning. The second part discusses how various perturbations of the excitation process of the spherical systems result in non-spherical field distributions expected to give rise to luminous regions of a form that might be associated with observations of high altitude sightings. The final summary and discussion conclude that the predicted behavior of the *DC* spherical transmission line model and its perturbed versions appears to be compatible with observed characteristics of ball lightning phenomena and also with some of the typical behavior of luminous high altitude sightings besides ball lightning.

Throughout the paper the development is adhering strictly to basic field theory, with adherence to proper boundary conditions. Besides emphasis on simplicity, the theory distinguishes itself from earlier attempts to link ball lightning to electromagnetic phenomena in that no high frequencies are involved in the final lightning state, just stationary *DC* fields, except during the excitation process. A unique feature of the present approach is the recognition of parametric energy conversions associated with time limited atmospheric current discharges. In this conversion process the *DC* electric energy, originally stored in clouds, is transferred via magnetic energy associated with the conducting channel to electric energy stored in the spherical system, with breakdown and ionization in a localized strong field region at the center. From this viewpoint ball lightning, as well as high altitude sightings, might be looked upon as

a simple conversion process of *DC* energy stored in clouds to *DC* energy stored in a spherical system whose special geometry with high fields at the center give rise to the lightning phenomena.

2. The Free Space Spherical Transmission Line system

The spherical transmission line is the spherical equivalent of the regular two-wire transmission line in the sense that both satisfy the same form of partial differential equations. For the spherical line the wave equation expressed in matrix form follows directly from the symmetric version ($\partial/\partial\phi = 0$) of Maxwell's field equations in spherical coordinates *r, θ, T*.

$$\frac{\partial}{\partial T}\begin{bmatrix} re_\theta(r,\theta,T) \\ rh_\phi(r,\theta,T) \end{bmatrix} + \begin{bmatrix} 0 & 1 \\ 1 & 0 \end{bmatrix}\frac{\partial}{\partial r}\begin{bmatrix} re_\theta(r,\theta,T) \\ rh_\phi(r,\theta,T) \end{bmatrix} = \mathbf{0} \tag{1}$$

where the following specifications apply:

$$\begin{aligned} e_r = e_\phi &= 0 \qquad e_\theta(r,\theta,T) \neq 0 \\ h_r = h_\theta &= 0 \qquad h_\phi(r,\theta,T) \neq 0 \end{aligned} \tag{2}$$

The normalized time $T = ct$ is of dimension *m* (meter). The normalized magnetic field $h_\phi(r, \theta, T) = Z_0 H_\phi(r, \theta, T)$ has the dimension *volt/m,* the same as the electric field $e_\theta(r, \theta, T)$. The constants $c = 1/\sqrt{\mu_0\epsilon_0}$ is the velocity of light and $Z_0 = \sqrt{\mu_0/\epsilon_0}$ is the impedance of free space.

In addition to being functions of *r* and *T* the dependence of the field variables $e_\theta(r, \theta, T)$ and $h_\phi(r, \theta, T)$ on the *polar* angle θ is determined from Maxwell's equations by noting that the components e_r and h_θ are zero everywhere, according to assumption (2). Therefore, the following relations hold:

$$\begin{aligned} (\nabla \times \vec{\boldsymbol{h}})_r &= \frac{1}{r\sin(\theta)}\frac{\partial}{\partial\theta}[r\sin(\theta)h_\phi(r,\theta,T)] = \frac{\partial e_r(r,\theta,T)}{\partial T} = 0 \\ \nabla\cdot\vec{\boldsymbol{e}} &= \frac{1}{r\sin(\theta)}\frac{\partial}{\partial\theta}[\sin(\theta)e_\theta(r,\theta,T)] = 0, \end{aligned} \tag{3}$$

from which we deduce

$$h_\phi(r,\theta,T) = \frac{\hat{\boldsymbol{h}}_\phi(r,T)}{\sin(\theta)} \qquad e_\theta(r,\theta,T) = \frac{\hat{\boldsymbol{e}}_\theta(r,T)}{\sin(\theta)} \tag{4}$$

which are true for all polar angles θ except for $r\sin(\theta) = 0$, i.e., on the *z*-axis, where the magnetic as well as the electric field are singular. We shall later come back to the singularity problems and how they are accounted for. For convenience we have introduced new field variables $\hat{e}_\theta(r, T)$ and $\hat{h}_\phi(r, T)$ which are independent of the polar angle θ. Thus, by simply implementing the common factor $\sin(\theta)$ in the final solutions according to Equation 4, the differential

Equation 1 is reduced to the following form containing only the independent variables r and T, but not θ:

$$\frac{\partial}{\partial T}\begin{bmatrix} r\hat{\boldsymbol{e}}_\theta(r,T) \\ r\hat{\boldsymbol{h}}_\phi(r,T) \end{bmatrix} + \begin{bmatrix} 0 & 1 \\ 1 & 0 \end{bmatrix} \frac{\partial}{\partial r}\begin{bmatrix} r\hat{\boldsymbol{e}}_\theta(r,T) \\ r\hat{\boldsymbol{h}}_\phi(r,T) \end{bmatrix} = \mathbf{0} \tag{5}$$

The differential form (Equation 5), representing the basic wave equation in spherical coordinates, is identical to the corresponding equation for a two-wire *T*ransverse *E*lectric *M*agnetic (*TEM*) dispersionless transmission line, the only difference being that the radial coordinate r replaces the longitudinal coordinate z in regular transmission lines, and that the field variables are inversely proportional to r. This perfect similarity implies that Equation 5 can be interpreted as representing an electrodeless spherical transmission line in free space, with the configuration analyzed by means of formulations, concepts, and results inherited from regular dispersionless transmission line theory.

The spherical system (r, ϕ, θ) dealt with in the present paper, distinguishes itself by having its cross section (the polar θ-direction) extending all the way from $\theta = 0$ to $\theta = \pi$. In this sense the cross section is infinite, with the fields satisfying Equations 4 and 5 in the entire cross section, except on the "infinite" boundary, the z-axis, where the fields are singular and need special consideration. We shall demonstrate that the singularity problem is resolved through processes associated with the discharge phenomenon itself, during the excitation process by the current in the conducting channel and in the aftermath of the strike by remnants of the original charges in the clouds. Furthermore, we shall show that the input and output ends of the finite length spherical transmission line are terminated by fields that are different from the basic transmission line fields. Thus, we are dealing with a realizable solution of Maxwell's equations consisting of spherical waves of "infinite" cross section with all boundary conditions satisfied. And as pointed out these will be of the stationary *DC* type.

2.1. Field Solutions in the Spherical Transmission Line

Equation 5 is readily solvable by diagonalization, a procedure resulting in the general field solutions

$$\begin{aligned} e_\theta(r,\theta,T) &= \frac{1}{r\sin(\theta)}[V_f(r-T) - V_b(r+T)] \\ h_\phi(r,\theta,T) &= \frac{1}{r\sin(\theta)}[V_f(r-T) + V_b(r+T)] \end{aligned} \tag{6}$$

where the functions $V_f(r-T)$ and $V_b(r+T)$ are *arbitrary* functions of $r-T$ and $r+T$, respectively, each with dimension volt. The dependence $\sin(\theta)$ on the polar angle θ has been added according to Equation 4.

The general solution (Equation 6) specifies the field components as superpositions of two pulses of arbitrary shape propagating without change of

shape with the velocity of light in the outwards and inwards radial direction, respectively. The arbitrary shapes of the pulses reflect the dispersionless character of the transmission line Equation 5, meaning that any frequencies including the time independent state, the *DC* state, are equally permitted. Because Equation 6 is the general solution of Equation 5, it must contain *all* possible solutions having the prescribed symmetry of the basic set of Equation 2. Solutions containing either $V_f(r-T)$ or $V_b(r+T)$ alone represent *radiation* in the $+r$ and $-r$ directions, respectively. Superpositions of an equal amount of both pulses form generalized spherical *standing waves*. Of these, the often overlooked time independent *DC* state represents a special stationary case playing a fundamental role in the proposed theory. This particular condition is seen to be satisfied when the two pulses $V_f(r-T)$ and $V_b(r+T)$ are both of *constant* shape independent of r and T. In this special case the solutions are certainly stationary, because neither $e_\theta(r, T)$ nor $h_\phi(r, T)$ depend on r and T, except for the trivial factor $1/r$. Accordingly, the conditions specifying static *electric fields* and static *magnetic fields* follow directly from Equation 6:

Static electric fields:

$$V_f(r-T) = -V_b(r+T) = -V_{b,0} = V_{f,0} \qquad e_\theta(r,\theta) = -\frac{2V_{b,0}}{r\sin(\theta)} \tag{7}$$

Static magnetic fields:

$$V_f(r-T) = V_b(r+T) = V_{b,0} = V_{f,0} \qquad h_\phi(r,\theta) = \frac{2V_{b,0}}{r\sin(\theta)} \tag{8}$$

where the constants $V_{b,0}$ and $V_{f,0}$ do not depend on r and T, but still must be interpreted as the amplitudes of spherical pulses propagating with the velocity of light in the sense that they are part of the general solutions (Equation 6) of the wave Equation 5. These particular *DC* solutions are not unique for the spherical transmission line but apply to regular transmission lines, for instance lossless parallel wires, described in any textbook on the subject. The static electric case (Equation 7) corresponds to the line being open at both ends and charged to a constant voltage V_0. The static magnetic case (Equation 8) corresponds to the line being fed at the input with a constant current generator and shorted at the output end.

The wave impedance Z_w of the outward and inward traveling radial pulses follows directly from Equation 6:

$$Z_w = \frac{e_\theta(r,\theta,T)}{H_\phi(r,\theta,T)} = Z_0\frac{e_\theta(r,\theta,T)}{h_\phi(r,\theta,T)} = \pm Z_0 \tag{9}$$

showing that the wave impedance is equal to the free space impedance Z_0, with the two signs applying to outward and inward pulses, respectively. The result is in agreement with the interpretation of the circuit as a spherical dispersionless transmission line with characteristic impedance Z_0.

In the basic form of Equation 6, the field solutions are valid in all space except on the boundary represented by the z-axis, but as expected we shall find that the spatial length of the spherical transmission line is limited to a finite region of r defined by $r_0 \leq r \leq r_{\max}$, where the lower limit r_0 defines a small region around $r = 0$, and the maximum limit $r_{\max}$ reflects the finite length of the charge release over which excitation takes place during a thunder strike or discharge. Above $r_{\max}$, the fields decay faster than $1/r$, so that this region is non-propagating, containing stored electromagnetic energy and therefore representing a distributed susceptance serving as end termination for the spherical transmission line causing complete reflection at this end.

In the excitation process, described in the next section, the magnetic field singularity is compensated by the current in the *active* source channel, which also specifies the location in space of the circuit's z-axis, (see Figures 1 and 2). During the *response* process, following the end of the discharge, the electric field singularity on the z-axis is compensated by charges originating in the discharge channel.

2.2. Excitation of the Transmission Line by Atmospheric Discharges

The excitation source is supposed to be the current arising from an atmospheric discharge shown in Figure 1. The strike between an electrified cloud and ground is likely to be a possible cause of observed ball lightning near ground, whereas intracloud lightning between charged clouds might be the source of higher atmospheric light phenomena. Except for the different locations and for the somewhat different boundary conditions near ground, the circuit responses in the two cases are expected to be similar. The location in space of the atmospheric discharge is expected to specify the circuit's initial position, with $r = 0$ at the symmetry point of the discharge string. If the discharge takes place between two clouds, the symmetry point is somewhere near the midpoint. With a typical cloud to ground discharge, claimed to initiate ball lightning, a reasonably well conducting ground plane defines the symmetry point $r = 0$ to be at or near ground level.

The electromagnetic processes associated with atmospheric discharges are fairly complex, as for instance shown in Uman (1987). Mathematical tractability calls for a simplified discharge model, which is taken to be a thin straight column of current shown in Figure 2.

The typical thickness of the column is 0.2 meters and the current averages 30,000 ampere. The discharge current $I(t)$ over the length L between clouds begins at time $t = t_0$ and lasts a short but finite time Δt until $t = t_1 = t_0 + \Delta t$ where the pulse duration Δt typically is of the order of one millisecond. During the discharge the current is not expected to be constant along the channel and not constant over the pulse length Δt, but for our purpose it suffices to assume the simple model of constant $I(t)$ over the interval. In view of the complex nature of lightnings the assumption of constant $I(t)$ is somewhat of an oversimplification,

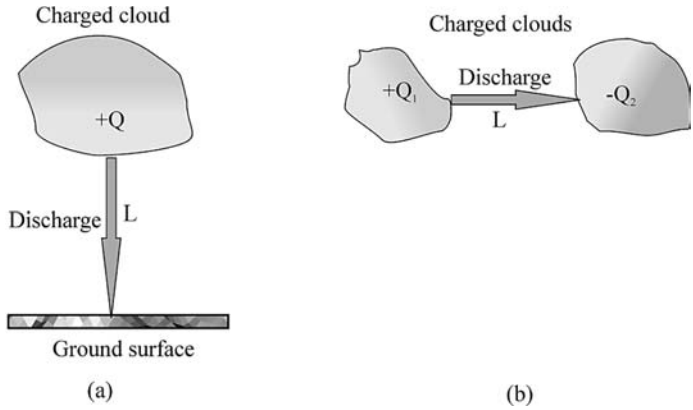

Fig. 1. Two kinds of atmospheric discharges: (a) Regular lightning between a charged cloud and ground. (b) Intracloud lightning between two clouds.

but is nevertheless thought to represent an adequate modeling of the source of ball lightning as well as higher altitude sightings, because we shall link these phenomena to the *time average current component,* which is guaranteed to be non-zero in discharge processes between oppositely charged clouds, regardless of the complexity of the discharge. In the analysis of the system the discharge column is regarded as an antenna fed by the current pulse I_0 of duration Δt. Part of the original electrostatic energy, built up before the strike, is *dissipated* inside the strike itself and in the ground, part of it is *radiated* into free space, and part of it is stored as magnetostatic energy around the strike. But the radiated part must be quite small. This statement follows from considering the frequency components $I(\omega)$ of the constant current pulse of length Δt*:*

$$I(\omega) = \frac{I_1}{2\pi} \frac{\sin(\omega \Delta t/2)}{\omega \Delta t/2} \tag{10}$$

With Δt equal to one millisecond, most of the frequency components of $I(\omega)$ are contained below 1000 Hz where the radiation efficiency of the channel, being roughly proportional to ω^2 is very low. This conclusion agrees with the fact that radio noise interference during thunderstorms is quite small in view of the enormous energy released. Therefore, during the strike the major part of the energy in excess of the dissipated energy is expected to be stored as non-radiative *magnetostatic DC* energy around the lightning bolt. In spiky types of discharges there could of course be any kind of high frequency components in addition to those specified by Equation 10, but the time average current is always non-zero in all discharges between oppositely charged clouds.

Therefore, in this model the high frequency components are negligible, and the magnetic field $H_\phi(r, \theta)$ can be evaluated by assuming a constant *DC* current equal to I_0. From general electromagnetic theory, the contribution $dH_\phi(r, \theta)$ to

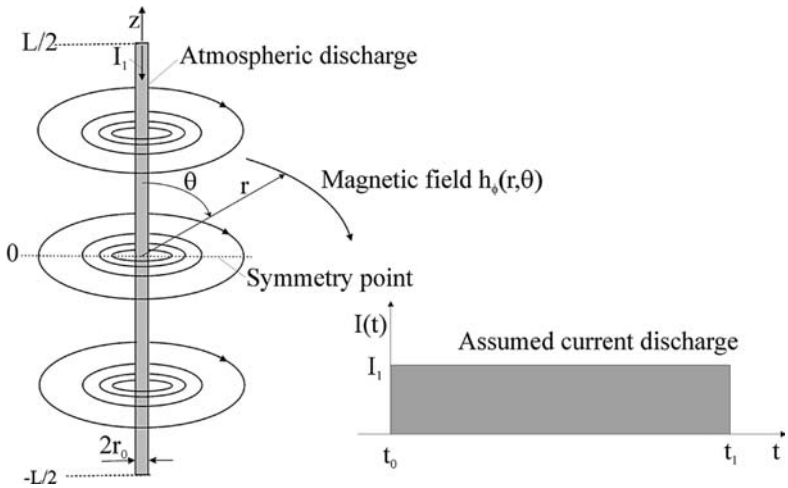

Fig. 2. Assumed model of the lightning bolt as a linear discharge column of length L, diameter $2r_0$, and constant current I_0.

the *DC* magnetic field at the coordinates (r, θ) from a small current element $I_0 dz$ is given by

$$dH_\phi(r,\theta) = \frac{I_0 dz}{4\pi r^2}\sin(\theta) \tag{11}$$

The overall magnetic field $H_\phi(r, \theta)$ from a discharge channel of length L is calculated by integration from $-L/2$ to $L/2$ resulting in the following formula:

$$H_\phi(r,\theta) = \frac{I_0}{2\pi r \sin(\theta)} f(R,\theta) \tag{12}$$

where the dimensionless factor $f(R, \theta)$ is a function of the normalized radius $R = r/(L/2)$ and the polar angle θ:

$$f(R,\theta) = \frac{1}{2}\left\{\frac{1 - R\cos(\theta)}{\sqrt{1 + R^2 - 2R\cos(\theta)}} + \frac{1 + R\cos(\theta)}{\sqrt{1 + R^2 + 2R\cos(\theta)}}\right\} \tag{13}$$

In Figure 3 the factor $f(R, \theta)$ is plotted as a function of $R = r/(L/2)$ with θ as parameter. The factor describes the magnetic field distribution as function of the length L of the discharge channel. In the limit of small L:

$$\lim_{L\to 0}[H_\phi(r,\theta)] = \frac{I_0 L}{4\pi r^2}\sin(\theta) \tag{14}$$

which corresponds to Equation 11, as expected. If L is infinite $f(R, \theta) \to 1$ so that the limiting magnetic field is given by

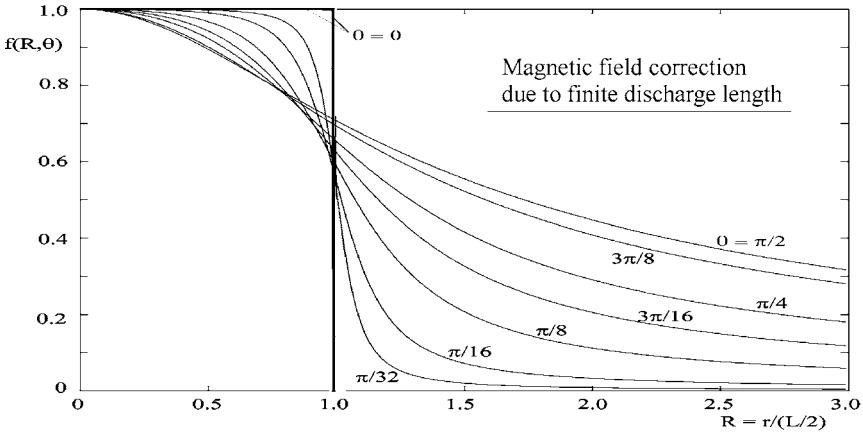

Fig. 3. Distribution of magnetic field around the discharge column of length L and constant current shown in Figure 2, expressed by the factor $f(R, \theta)$ as function of normalized radius $R = r/(L/2)$ with θ as parameter.

$$H_\phi(r, \theta) = \frac{I_0}{2\pi r \sin(\theta)} \tag{15}$$

which is exactly the characteristic *DC* magnetic field (Equation 8) of the spherical transmission line excited in the magnetic mode. Hence we may conclude that the dominating *DC magnetic component* of a discharge channel of infinite length is a perfect source of *DC* magnetic excitation of the spherical transmission line. Additional excitations due to higher frequency current components in the discharge are expected to be negligible and are disregarded.

If the discharge channel deviates from the straight model assumed in Figure 2, a more general approach to the excitation process must be used. From general electromagnetic theory, described for instance in Wessel-Berg (2000), the excitation of the magnetic field of the spherical transmission line is specified by a coupling integral over space of the *driving* magnetic field (Equation 12) weighed against the *characteristic* magnetic field (Equation 8) of the line. Microwave tube scientists will recognize this as a generalization of Ramo's theorem (Ramo, 1939) for calculation of induced currents in microwave devices. The method demonstrates that also quite complex discharges give rise to some excitation of the spherical system, with magnitude determined by the details of the lightning strike through a corresponding coupling integral.

In real atmospheric discharges the discharge length L is of course not infinitely long so that the factor $R = r/(L/2)$ is larger than zero, with only partial coupling to the spherical system. From the shape of the curves it is concluded that the main contribution to the coupling integral comes from the region below $R \approx 1$, i.e., $r \approx L/2$. Above this value the magnetic field decays faster than $1/r$, and does not represent spherical traveling wave components with constant power

independent of r. Therefore, the region above $r \approx L/2$ is interpreted as a *distributed susceptance* serving as termination of the transmission line. For the purpose of mathematical simplification without undue loss of accuracy, the absence of a well-defined point of reflection is accounted for by defining a *nominal* transmission line length $r_{\max}$ based on the factor $f(R, \theta)$. The nominal length is taken to be

$$r_{\max} = \frac{L}{2} \tag{16}$$

which implies the following approximation of $f(R, \theta)$:

$$f(R, \theta) \approx 1 \quad \text{for } R \leq 1. \tag{17}$$

The selection implies a simple model in which the spherical transmission line extends from r_0 to $r_{\max} = L/2$ where it is terminated with a *localized* susceptance equivalent to the actual distributed susceptance. Although the model is approximate, it is believed to be an adequate representation of the process.

In order to reap the full benefits of the transmission line model we must describe the stationary magnetic field in terms of the appropriate variables (Equation 8) defined earlier for this model. This is a straightforward process specifying the two constant pulses $V_f(r - T) = V_{f,0}$ and $V_b(r + T) = V_{b,0} = V_{f,0}$ superposed with equal amplitudes to yield zero electric field but non-zero magnetic field, as shown in Figure 4a. During the initial stage of the interval Δt the outward propagating pulse $V_f(r - T)$ travels with the speed of light to the nominal maximum radius $r_{\max}$ where it is completely reflected into the inward pulse $V_b(r + T)$. At $r = r_0$ the process repeats itself, with $V_b(r + T)$ reflecting into $V_f(r - T)$, thus completing the round trip. The time it takes to complete the round trip is negligible compared to the pulse duration Δt.

Thus, at the end of this sequence, illustrated schematically in Figure 4a, the entire circuit volume from $r = r_0$ to $r = r_{\max}$ is filled with magnetic energy consisting of two superimposed oppositely traveling components of constant magnitude $V_{f,0} = V_{b,0}$ representing a standing *DC* magnetic wave of constant amplitude (except for the $1/[r \sin(\theta)]$ variation).

$$e_\theta(r, \theta) = 0 \qquad H_\phi(r, \theta) = \frac{2V_{b,0}}{r \sin(\theta)} \tag{18}$$

The stored magnetic energy beyond $r = r_{\max}$ represents a distributed susceptance, providing complete reflection of the outward traveling wave. The described process is analogous to propagation on a shorted two-wire transmission line of length $r_{\max} - r_0$ fed at the input end by a *DC* current generator of constant current I_0.

This semi-stationary situation changes dramatically with the abrupt discontinuation of the driving current at $t = t_1$. In the parlance of electromagnetic theory this is interpreted as a *parametric process* because the electromagnetic parameters of the system changes due to the abrupt expiration of driving current

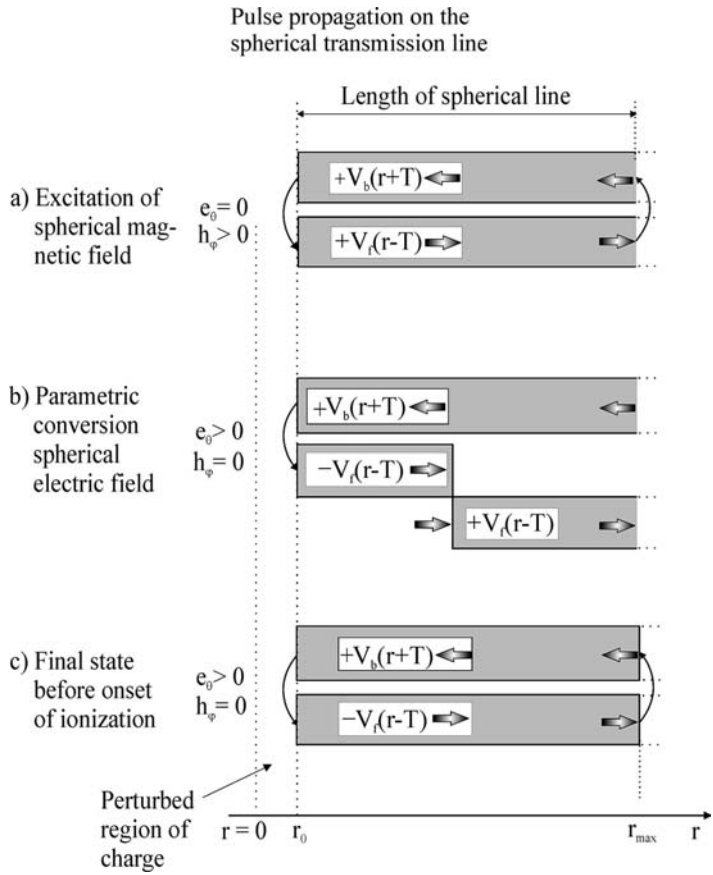

Fig. 4. Illustration of the parametric conversion from magnetic to electric energy storage. (a) Magnetic storage expressed by two oppositely traveling *DC* pulses along the spherical transmission line. (b) Transient conversion from magnetic to electric energy at the end of the lightning bolt. (c) Final stationary state before onset of the ionization process.

in the conducting channel. The advantage of the transmission line formulation in handling the appropriate non-stationary response to this parametric phenomenon will soon be apparent.

2.3. The Parametric Process of Energy Conversion

With the sudden termination of the driving current $I(t)$ at the end of the strike at time t_1 the stationary situation described above and depicted in Figure 4a changes quite dramatically, as further illustrated in Figure 4b. The response of the circuit must still be described uniquely by pulses $V_b(r+T)$ and $V_f(r-T)$, because these are the *general* solutions of the differential Equation 5.

The termination of driving current $I(t)$ is immediately followed by a gradual disappearance of the magnetic field, beginning at $r = r_0$. The pulse component $V_f(r - T)$ reverses its sign so that the net magnetic field at $r = r_0$ switches from its original finite value to zero, whereas the electric field e_θ is no longer compensated but switches from zero to a finite value.

The transient state described in Figure 4b is further illustrated in Figure 5 showing the expanding electric field $e_\theta(r, \theta)$ and the corresponding channel current which is gradually reduced to zero along the line, being replaced by constant charges $+Q$ and $-Q$ specified by

$$Q(z) = 4\pi\epsilon_0 V_{f,0} \frac{z}{|z|} \tag{19}$$

The constant charges of opposite signs, matching the electric field on the z-axis, are drawn from the ionized channel at the abrupt interfaces between $I(t) = 0$ and $I(t) = I_0$ during the transient process. The central region is presumably excluded from the process and must be assumed free of charges. As shown in Figure 5 the accumulation of positive and negative charges in the upper and lower part of the channel is a result of currents due to the z-component of the electric field along the axis, obtained from the relation

$$E_z(r, \theta) = e_\theta(r, \theta) \sin(\theta) = \frac{2V_{f,0}}{r \sin(\theta)} \sin(\theta) = \frac{2V_{f,0}}{r} \tag{20}$$

Due to higher mobility of electrons, electrons dominate the corresponding current. As a result, negative charges flow into the upper half and out of the lower part of the channel, creating the gradual buildup indicated in Figure 5. By their nature the compensating charges tend to offset the basic field distribution and, besides introducing some uncertainty about the extension $r_{\max}$ of the circuit, might play a role in forming ionized regions differing from the spherical shape, as discussed in Section 3.4. The fields on the z-axis beyond $z = \pm L/2$, i.e., beyond the actual transmission line, are not singular and therefore in no need of free charges, a feature attributed to the fact that the radial field in this region decays more rapidly than $1/r$.

The overall parametric process is seen to be a gradual conversion of magnetic field energy to electric field energy, beginning at $r = r_0$ and propagating outward with the velocity of light in the form of a radially expanding spherical pulse $-V_f(r - T)$, until the nominal outer circuit radius $r_{\max}$ where full conversion is achieved. This marks the end of the transient non-stationary state depicted in Figure 4b and Figure 5. From that time on the circuit is again in a stationary *DC* state with the original magnetic field distribution $h_\phi(r, \theta)$ of Figure 4a replaced completely by the electric field distribution $e_\theta(r, \theta)$ shown in Figure 4c. The properties of this state are summarized as follows. The *DC* pulses $V_f(r - T) = -V_{f,0}$ and $V_b(r + T) = V_{b,0}$ are equal with the opposite sign so that $V_{f,0} + V_{b,0} = 0$ and therefore

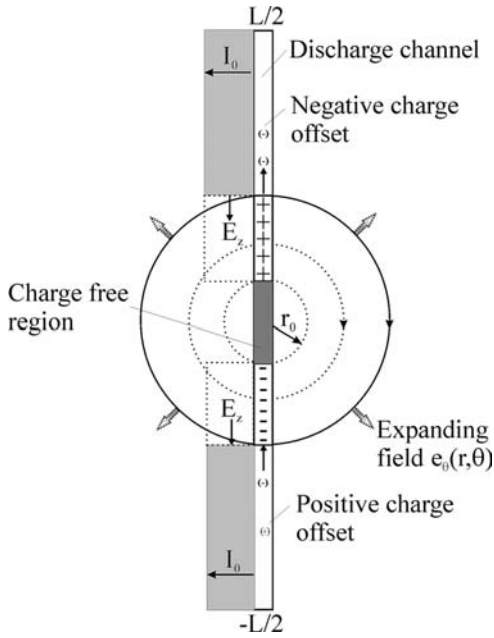

Fig. 5. Details of the transient process shown in Figure 4b, showing an intermediate state with the expanding electric field $e_\theta(r,\ \theta)$, the corresponding decay of current in the discharge column, and the gradual buildup of charges replacing the current. Also note the gradual accumulation of charge offsets in the column.

$$H_\phi(r,\theta) = 0 \qquad e_\theta(r,\theta) = \frac{2V_{f,0}}{r\sin(\theta)} \tag{21}$$

Thus, in this parametric process the spherical transmission line, originally excited in a static magnetic field by the discharge, is completely converted to a *static* electric field along the spherical transmission line. The electric field, proportional to $1/r$, is very strong near the center and, in addition, singular on the z-axis. Therefore, in a central region around $r = 0$ the electric field strength is expected to cause ionization of the air.

2.4. Total Reflections at Both Ends

The standing wave of *DC* electric field requires terminations of the spherical transmission line causing complete reflections at $r = 0$ and $r = r_{\max} \approx L/2$. The nominal point of reflection $L/2$ is not exact, but represents an approximation allowing a simple mathematical treatment without sacrificing the essentials of the physical process. In this model the end point of the line is terminated in a pure susceptance Y that always gives a reflection coefficient ρ of magnitude unity:

$$|\rho| = \left|\frac{Y-1}{Y+1}\right| = 1 \tag{22}$$

causing total reflection.

In reality, the reflection occurs continuously over the entire length of the *finite* line due to the deviation of the field from the perfect $1/r$ variation of the *infinite line*. Figure 7 shows the gradual change of standing wave electric fields from pure circular near $r = 0$ to a more elongated form at the end point and beyond, indicating deviation from the $1/r$ variation. In a lossless line the decay of radial power flux can only be accounted for by reflecting part of the power, expressed by a continuous reflection coefficient along the line. The reflections are due to a set of extra field components $e_\theta(r, \theta)$ and $e_r(r, \theta)$ having r-variation different from $1/r$. Following, for instance, Jackson (1975: chap. 3), the extra fields, which must be regular everywhere, including the z-axis, are specified by the general series

$$\begin{aligned} e_\theta(r,\theta) &= \sum_{l=1}^{l=odd}\left(a_l r^{l-1} + b_l \frac{1}{r^{l+2}}\right)\frac{dP_l[\cos(\theta)]}{d\theta} \\ e_r(r,\theta) &= \sum_{l=1}^{l=odd}\left[a_l l r^{l-1} - b_l(l+1)\frac{1}{r^{l+2}}P_l[\cos(\theta)]\right] \end{aligned} \tag{23}$$

where $P_l[\cos(\theta)]$ is the lth Legendre Polynomial of odd order. Selection of odd values of the index l assures that the field has the right symmetry:

$$e_\theta(r, \pi/2 - \theta) = e_\theta(r, \pi/2 + \theta) \tag{24}$$

The series form a *complete* set for expansion of any field distribution satisfying the stated symmetry criterion and being regular everywhere. The total reflections at the output end are implemented by the b_l series, with $a_l = 0$ for all l, matching any field distribution by appropriate choice of expansion coefficients b_l. For this series the radial variations are $1/r^3$, $1/r^5$ ..., confirming the absence of propagating terms $\sim 1/r$.

The total reflection at the input end is enforced by the a_l series with $b_l = 0$ for all l. Reflections simply have to occur because there exists no load into which the inward wave component $V_b(r - T)$ can be dissipated. The reflection is assumed to take place over some small region $0 < r < r_0$ in which the inward wave component proportional to $1/r$ is met by field components *decaying* towards $r = 0$ with a_l terms proportional to r^2, r^4 ... that can be matched to any finite field distribution by appropriate choice of expansion coefficients.

3. The Ionized State

The electric field is proportional to $1/r$ and therefore expected to cause ionization of the air up to a certain radius $r = r_i$, at which point the electric field becomes too small to sustain ionization. The breakdown field strength for

ionization of the air is of the order of 30,000 volts/cm at ground level and somewhat smaller at higher altitudes. The ionization process is in itself an exceedingly difficult subject, treated only superficially in the paper, which puts the emphasis on the underlying electromagnetic phenomena. The ionized region is considered to be a neutral plasma introducing small perturbation terms in the basic lossless spherical circuit. The perturbation terms are due to the flow of electron current caused by the basic *DC* field (Equation 21). In the presumably collision dominated ionized region the current is *solenoidal* everywhere, with $\nabla \cdot \vec{i} \approx 0$ and no net charges, in analogy with current flow in a metallic conductor. The electron mobility is presumably much higher than the ion mobility so that the current density is specified by

$$r\hat{i}_\theta(r) = \sigma r\hat{e}_\theta(r) = \sigma 2V_{f,0} = \text{constant} \tag{25}$$

where σ is the electron mobility assumed to be constant over the entire ionized region.

$$\sigma = \frac{q^2 n_e}{\omega_{col} m_e} \tag{26}$$

Here, q is the electron charge, m_e and n_e electron mass and density, respectively, and ω_{col} collision frequency. In an ionized plasma the conductivity σ representing the collision frequency is a macroscopic parameter specifying the combined effect of thermal loss, i.e., heating, and emission loss. The question which of the two is dominating is left open in this paper, although ball lightning observations seem to indicate fairly low heating effect.

The associated magnetic field due to the current is obtained from Maxwell's second equation, noting that $\partial/\partial T = 0$ under *DC* conditions.

$$\frac{\partial}{\partial r}[r\hat{h}_\phi(r)] + Z_0 r\hat{i}_\theta(r) = 0 \tag{27}$$

Insertion from Equation 25 converts the equation to

$$\frac{\partial}{\partial r}[r\hat{h}_\phi(r)] = -Z_0\sigma 2V_{f,0} = \text{constant} \tag{28}$$

which is solved by direct integration:

$$r\hat{h}_\phi(r)_{bulk} = -2Z_0\sigma V_{f,0} r \tag{29}$$

The equation shows that this component of magnetic field $r\hat{h}_\phi(r)_{\text{bulk}}$ inside the ionized region increases *linearly* with radius r. There is an additional component caused by *the axial* current $I_z(z)$ arising from current continuity requirement $\nabla \cdot \vec{i} \approx 0$ at or near the z-axis, obtained as follows. The current component normal to the axis is given by

$$\lim_{a\to 0}(2\pi a i_{rad}) = \lim_{a\to 0}(2\pi\sigma a e_\theta) = \frac{\sigma}{\epsilon_0}Q(z) \tag{30}$$

where $Q(z)$ is the on axis charge accumulation given by Equation 19. The equation of continuity is then

$$\frac{\partial I_z(z)}{\partial z} + \frac{\sigma}{\epsilon_0} Q(z) = 0 \tag{31}$$

Separate integration over the upper and lower half where Q is constant results in

$$I_z(z) = \frac{\sigma}{\epsilon_0} |Q|(r_i - |z|) \tag{32}$$

where the constants of integration are selected to render the axial current zero at the ionized boundary $z = \pm r_i$. The current is maximum at $z = 0$, decaying linearly towards $z = \pm r_i$. The axial current serves as the return path of the bulk current impinging on the axis, thereby producing a magnetic field component opposite the bulk component (Equation 29). An estimate of the magnetic field H_ϕ due to $I_z(z)$ is obtained using the simple approximation $2\pi r \sin(\theta) H_\phi = \langle I_z(z) \rangle$ where $\langle I_z(z) \rangle = \sigma |Q| r_i / \epsilon_0$ is the average current, resulting in the approximate formula:

$$r\hat{\boldsymbol{h}}_\phi(r)_{axial} = Z_0 \sigma V_{f,0} r_i \tag{33}$$

By additions of the contributions of Equations 29 and 33 the net magnetic field becomes

$$r\hat{\boldsymbol{h}}_\phi(r) = r\hat{\boldsymbol{h}}_\phi(r)_{bulk} + r\hat{\boldsymbol{h}}_\phi(r)_{axial} = -2Z_0 \sigma V_{f,0} \left(r - \frac{r_i}{2} \right) \tag{34}$$

Hence, in the central region $r < r_i/2$ the magnetic field due to the axial current prevails. After sign reversal at $r = r_i/2$ the bulk current dominates in the outer region $r_i/2 < r < r_i$. Therefore, at the boundary $r = r_i$ of the ionized region the magnetic field is given by

$$r_i \hat{\boldsymbol{h}}_\phi(r_i) = -Z_0 \sigma V_{f,0} r_i \tag{35}$$

Outside the ionized region, where the current is zero, the magnetic field is expected to decay as $1/r$ or faster. The inward looking normalized *DC* impedance of the glossy ionized region is then

$$Z_i = \frac{r_i \hat{\boldsymbol{e}}_\theta(r_i)}{r_i \hat{\boldsymbol{h}}_\phi(r_i)} = \frac{2}{Z_0 \sigma r_i} \gg 1 \tag{36}$$

The real impedance Z_i at the ionized boundary r_i serves as a load, causing a periodic discharge of the stored energy of the transmission line outside the region. The details of the process are identical to the discharge of a two-wire transmission line through a resistor at the end, explained in any textbook on the subject. The result of the process is that the fields in the ionized region go through a decaying sequence of intermediate stationary states. The stationary state is a consequence of having most of the circuit energy stored *outside* the

ionized region, so that the behavior is dominated by the two external pulses $V_b(r+T)$ and $V_f(r-T)$ along the line. Let us direct attention to the transition from the non-ionized to ionized state, whereby the situation in Figure 4c changes to that of Figure 6a. The ionization process taking place for $r \leq r_i$ has no effect on the already existing external pulse $V_b(r+T)$ that continues its inward propagation into the ionized zone. At the interface $r = r_i$ all fields are continuous, so that the inside electric field is forced to take on the same value as that of $V_b(r+T)$. And this situation persists during the round-trip transit time $\Delta T = 2(r_{\max} - r_i)$ of the reflected outward pulse $V_f(r-T)^{(1)}$, which is reduced slightly due to the change of impedance at the interface, according to:

$$V_f(r-T)^{(1)} = -\rho V_b(r+T)^{(0)} \tag{37}$$

where the reflection coefficient ρ is given by

$$\rho = \frac{Z_i - 1}{Z_i + 1} \tag{38}$$

Due to the ionization, the normalized impedance Z_i is not infinite but still expected to be much larger than unity, so that ρ is slightly less than unity. Thus, when the outward pulse $V_f(r-T)^{(1)}$, now slightly reduced in magnitude, reaches the outer nominal radius $r_{\max}$ it is reflected into an inward pulse $V_b(r-T)^{(1)}$, which is also slightly reduced in size compared to the previous $V_b(r+T)^{(0)}$, The inward pulse then hits the interface at r_i after an overall normalized time expenditure $\Delta T = 2(r_{\max} - r_i) \cong 2r_{\max}$. The requirement of continuity at the interface causes a reduction of the electric field from $r\hat{e}_\theta^{(0)}$ to $r\hat{e}_\theta^{(1)}$ specified by

$$r\hat{\boldsymbol{e}}_\theta(r)^{(1)} = \rho r\hat{\boldsymbol{e}}_\theta(r)^{(0)} \tag{39}$$

After this first round-trip sequence the process repeats itself successively, as illustrated in Figure 6b and c. The process continues until the field strength falls below the breakdown field strength, at which point ionization is extinguished and light emission ceases.

3.1. Superimposed High Frequency Fields

The described process, in which the fields and currents in the ionized region are specified as a sequence of stationary states, is not a mathematical approximation, but a real physical phenomenon. The abrupt transitions from one state to the next is a periodic phenomenon with periodicity $\Delta t = 2r_{\max}/c$ giving rise to a high frequency field component of fundamental frequency f_0 specified by

$$f_0 = \frac{1}{\Delta t} = \frac{c}{2r_{\max}} \tag{40}$$

The corresponding fundamental wavelength λ_0 is equal to $2r_{\max}$. The high frequency fields associated with this phenomenon are superimposed on the *DC* state described in the foregoing sections as a small perturbation. Accordingly,

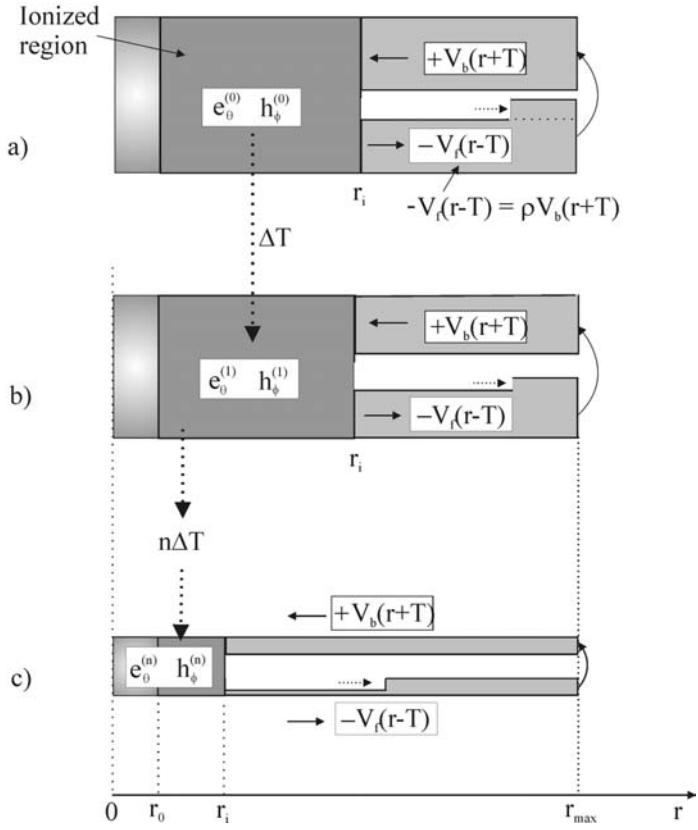

Fig. 6. Illustration of the sequential decay of stored energy in the ionized region. (a) Situation immediately after onset of ionization, showing the reduced amplitude of the outward pulse $V_f(r-T)$. (b) The same, after one more round-trip of time $\Delta t = \Delta T/c$. (d) The same, after n round-trips $n\Delta t$, just prior to extinction of ionization.

we shall take the outward appearance of the ionized region to be a localized circuit with basic high electric *DC* fields and small superimposed perturbations caused by a finite conductivity σ giving rise to *DC* current flow, associated magnetic field, and small superimposed *R*adio *F*requency (*RF*) fields of fundamental frequency f_0 all field components decaying exponentially with respect to time, as described in the next section.

3.2. Decay Rate and Lifetime

The transit time $\Delta t = \Delta T/c$ is extremely short, so that for all practical purposes the described process can be considered to be continuous. A course estimate of the decay rate is obtained by considering two subsequent states separated in time by the overall normalized transit time $\Delta T \approx 2r_{\max}$:

$$\frac{d[r\hat{e}_\theta(r)]}{dT} = \frac{r\hat{e}_\theta(r)^{(n)} - r\hat{e}_\theta(r)^{(n-1)}}{\Delta T} = \frac{\rho - 1}{2r_{\max}} r\hat{e}_\theta(r)^{(n-1)} \tag{41}$$

Expressed in real time the equation is solved by

$$\hat{e}_\theta(r,t) = \hat{e}_\theta(r,t_0)\exp\left(-\frac{t-t_0}{\tau}\right) \tag{42}$$

where the time constant τ is given by

$$\tau = \frac{2r_{\max}}{(1-\rho)c} = \frac{r_{\max}}{r_i c}(Z_i + 1) \cong \frac{\varepsilon_0}{\sigma}\frac{r_{\max}}{r_i} \tag{43}$$

According to Equation 43 the time constant τ is determined from the conductivity σ and the circuit size expressed by $r_{\max}$ and r_i. Because of the many uncertainties concerning the conductivity parameter σ, in particular its variation over the region and possible non-linearity, the numeric value of lifetime obtained from the formula is not expected to be very accurate.

The proportionality of τ with $r_{\max}$ is merely demonstrating the proportionality of the time constant with stored energy, which is gradually dissipated in the ionized ball, all very similar to a high Q resonant circuit with small loss. The nature of the process is a slow decay in which only some fraction of the available energy has been lost at the end of the ball lightning, with perhaps most of the energy remaining in the spherical circuit, but with insufficient field strength to cause ionization and ball lightning.

The decay of fields (Equation 42) is associated with a corresponding decay of stored energy $W(t)$ having twice the decay rate.

$$W(t) = \exp\left[\frac{-2(t-t_0)}{\tau}\right] W(t_0) \tag{44}$$

In the decay process the energy is gradually dissipated in the ionized region and converted to heat and emitted light with an expected increase in temperature of the ionized air, referred to as the ''hot balloon effect,'' a phenomenon that warrants particular attention, as discussed more thoroughly later.

Observations of typical ball lightning indicate lifetimes τ of the order of a few minutes or less. In addition to lifetime there are other observations relating indirectly to conductivity, namely absence of excessive heating of the ionized ball, a fact indicating a fairly low conductivity. Many higher altitude sightings indicate considerably longer lifetimes, a fact that might be attributed to larger stored energy.

3.3. Stored Energy

The energy density $w(r, \theta)$ as a function of θ is evaluated from *Poynting's* theorem, which in the present case takes the form

$$\frac{\partial \Delta p(r,\theta)_{\pm}}{\partial r} + c\frac{\partial w(r,\theta)}{\partial T} = 0 \tag{45}$$

where the power density $\Delta p(r, \theta)$ of two general pulses along the transmission line is given by

$$\Delta p(r,\theta) = \frac{2\pi}{Z_0 \sin(\theta)}\left[V_f(r-T)^2 - V_b(r+T)^2\right] \tag{46}$$

The subscript $\pm$ in Equation 45 indicates that the equation applies to either pulse, with energy contributions adding up. The fact that the pulse shapes are stationary implies that the energy density at some arbitrary position within the pulse is constant and moving in synchronism with the pulse. Therefore, the *total* time derivative of $w(r, \theta)$ must be zero. Expressed in the normalized time variable T:

$$\frac{dw(r,\theta)}{dT} = \frac{\partial w(r,\theta)}{\partial T} + \frac{\partial w(r,\theta)}{\partial r} = 0 \tag{47}$$

Combining Equations 45 and 47 we obtain

$$\frac{\partial}{\partial r}\left[\Delta p(r,\theta)_{\pm} - cw(r,\theta)\right] = 0 \tag{48}$$

Because the equation holds everywhere within an arbitrarily shaped pulse we must have $\Delta p(r, \theta)_{\pm} = cw(r, \theta)$, and therefore

$$w(r,\theta) = \frac{\Delta p(r,\theta)}{c} = \frac{2\pi}{cZ_0 \sin(\theta)}\left[V_f(r-T)^2 + V_b(r+T)^2\right] \quad [\text{joule/m}] \tag{49}$$

where the contributions from both pulses are added. The *total energy density* $w(r)_{\text{tot}}$ over the full range of the polar angle θ is obtained by integration over θ excluding a small conical region of angle δ around the z-axis, accounting for the small lateral extent of the charged region around the z-axis. The integral evaluates to

$$w(r)_{tot} = \int_{\delta}^{\pi-\delta} w(r,\theta)d\theta \;=\; -\frac{4\pi}{cZ_0}\left[V_f(r-T)^2 + V_b(r+T)^2\right]\log(\delta) \quad [\text{joule/m}] \tag{50}$$

The equation applies to the general case of arbitrary pulses $V_f(r-T)$ and $V_b(r+T)$ showing that the energy density $w(r)_{\text{tot}}$ is non-zero within the domains of the localized pulses. Because the pulses $V_{f,0} = V_{b,0}$ are constant in the present stationary *DC* state, the energy density $w(r)_{\text{tot}}$ is independent of r and given by

$$w(r)_{tot} = w_{tot} = -\frac{8\pi}{cZ_0}V_{f,0}^2\,\log(\delta) \quad [\text{joule/m}] \tag{51}$$

The total energy W in the transmission line of nominal length $r_{\max} = L/2$ is therefore given by

$$W = w_{tot} r_{\max} = -\frac{4\pi}{cZ_0} F_0^2 \, L \log(\delta) \quad [\text{joule}] \tag{52}$$

Through Equation 21 the *DC* pulse amplitude $V_{f,0}$ can be estimated from the required electric breakdown field $e_\theta(r_i)_{break}$ at the interface $r = r_i$.

$$V_{f,0} = \frac{1}{2} r_i \hat{e}_\theta(r_i)_{break} \tag{53}$$

so that relation (Equation 52) appears in the following form:

$$\frac{W}{\log(\delta)} = -\pi \frac{\hat{e}_\theta(r_i)_{break}^2}{Z_0} \frac{L r_i^2}{c} \quad [\text{joule}] \tag{54}$$

The proportionality between energy W and size $L = 2r_{\max}$ is a manifestation of the large volume of energy storage. This point is confirmed by the example quoted below in Equation 55.

The right hand side of Equation 54 contains the variable r_i that can be *observed* and the *known* ionization field variable $e_\theta(r_i)_{break}$ which for air at room temperature and atmospheric pressure is roughly equal to 3×10^6 volt/meters. Because the left hand factor $\log(\delta)$ is a very slow varying function of δ, the uncertainty associated with this factor is not serious, because the actual small value selected in the integration in Equation 50 has only a minor effect on the *order* of W. This is demonstrated by an example selecting the small conical angle δ equal to 0.0001 which gives $\log(\delta) = -9.2$. Reducing δ by a large factor of 10,000 causes $\log(\delta)$ to increase just by a factor of two. Therefore, Equation 54 provides an order of magnitude estimate between stored energy W and the length of the lightning bolt $L = 2r_{\max}$. Let us take two extreme examples of ionized size r_i, somewhat arbitrarily putting $\log(\delta) = -20$.

$$\begin{aligned} r_i &= 0.1 \quad [\text{m}] \qquad W \approx 50 L_{meter} \quad [\text{joule}] \\ r_i &= 10 \quad [\text{m}] \qquad W \approx 0.5 \cdot 10^6 L_{meter} \quad [\text{joule}] \end{aligned} \tag{55}$$

The first example represents a typical ball lightning observation, whereas the second one might be representative for higher altitude sightings.

From various observations quoted in the literature the energy stored in ball lightning has been estimated to be between 10^2 and 10^6 joule. For these values, Equation 55 estimates the corresponding discharge length L between 2 and 2000 meters. The wide range, although a very rough estimate, indicates that ball lightning perhaps might occur under many different discharge conditions. In particular, the prediction of the short discharge length of $L = 2$ meters associated with the lower energy raises the interesting question whether such short discharges are realistic alternatives. Rather than occurring in free space between clouds and ground, they might possibly occur under special kinds of electrical conditions in confined environments such as inside buildings or airplanes, a possibility supported by reported observations (Grigor'ev, Grigor'eva, & Shiryaeva, 1992). The second example in Equation 55 with large size $r_i = 10$

meters might perhaps be representative of higher altitude sightings, and involves considerably larger stored energy.

From Equation 40 the expected frequency of the time varying field superimposed on the *DC* field is 150 MHz for the shorter length of 2 meters and 15,000 Hz for $L = 20{,}000$ meters. Hence, in the high energy range audible acoustic vibrations may well be excited in the ionized sphere through non-linear coupling effects to ionized gas molecules, an effect that might possibly explain reported observations of ball lightning emitting a hissing sound.

The information gained from this example confirms the conceptual picture of ball lightning and higher altitude sightings as more than just a local phenomenon limited in size to the ionized region itself. By far most of the energy is contained outside, continuously feeding the ionized region where the energy is slowly dissipated until the field becomes too small for sustainable ionization.

3.4. Shapes of Ionized Regions

The solenoidal current density vector $\hat{\imath} = \sigma\hat{e}$ coincides with the electric field and also defines the boundary of the ionized region. If the boundary of the ionized region did not coincide with the direction of the field and the current, there would necessarily be a current component *crossing* the boundary between ionized and non-ionized air, causing the buildup of the equivalent of a surface charge distribution. This distribution would, in turn, give rise to its own electric field distribution tending to compensate the current flow across the boundary and serving to counterbalance the flow across the boundary, thereby tending to stabilize the surface in a form defined by the electric field lines. Therefore, for all the particular shapes of field line distributions discussed in the following, the ionized region is expected to coincide with the field lines. The ionized gas inside the region is expected to emit visible light which we shall tentatively identify with ball lightning or with higher altitude light phenomena.

In particular, in the basic model of the spherical circuit the ionized region is expected to be spherical, coinciding with the $e_\theta(r_i)$ field line, in spite of the fact that the field varies as $1/\sin(\theta)$ and therefore is much stronger near the z-axis. However, the basic model is somewhat oversimplified in that the spherical shape of fields is strictly true only for an infinite length L of the original discharge column. For more realistic finite lengths the fields are expected to deviate somewhat from the spherical shape although we expect the basic $1/r$ characteristic to be essentially retained so that localized ionization may still take place. In particular we shall investigate the effect of different distributions of the charge buildup on the z-axis during the conversion process from pure magnetic to electric energy, depicted earlier in Figures 4 and 5.

The illustrations shown below are obtained by *assuming* a specified finite length and charge distribution on the z-axis and calculating the electric field resulting from the charge. Figure 7 refers to the case of a finite length circuit with $L = 200$ meters and with the $+Q$ and $-Q$ charge densities on the upper and

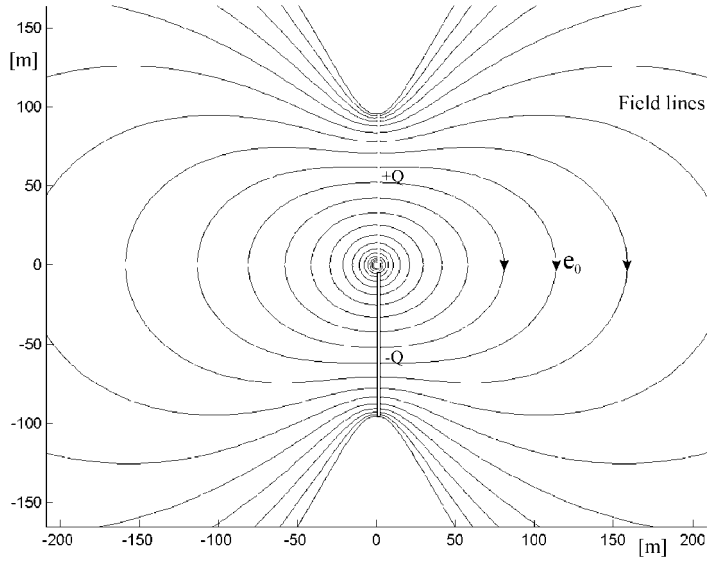

Fig. 7. Illustration of elongation of electric field lines due to a finite length discharge column of $L = 200$ meters.

lower part of the z-axis meeting at $z = 0$. Except for the region close to the center, which retains the spherical field shape, the immediate effect is an elongation of the field distribution in a direction normal to the z-axis. If the ionization extends beyond the central region, the expected shape would be more like a disk rather than spherical.

If the charge columns do not meet at the center but are separated a small distance, the field distribution in the central region is affected accordingly, with the fields directed predominately in the direction of the z-axis, as demonstrated in Figure 8 and in the expanded version of Figure 9. If ionization were limited to the central part, this particular case would result in a cigar-shaped ionized region.

In the discussion in connection with the more detailed sketch of Figure 5, attention was drawn to the likely creation of compensating charges of opposite sign along part of the length. In the following example each half of the overall column contains both positive and negative charges, according to:

$$\begin{array}{cc} \text{Upper half} & \text{Lower half} \\ 0 < z < L/4\text{: Charge} = +Q & -L/4 < z < 0\text{: Charge} = -Q \\ L/4 < z < L/2\text{: Charge} = -Q & -L/2 < z < -L/4\text{: Charge} = +Q \end{array} \qquad (56)$$

As shown in Figure 10, such a semiperiodic charge configuration has a major influence on the field distribution. First of all, the normal constant direction of the polar e_θ-field is reversed at some radius $r \approx L/4$, leaving an approximately field-

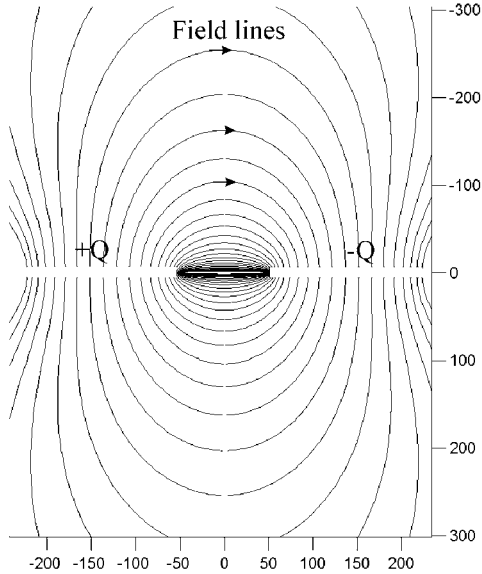

Fig. 8. Field distribution obtained with a charge column of 500 meters, with a 100-meter separation gap at the center. The cigar-shaped field distribution at the center is shown magnified in Figure 9.

free zone outside the strong fields in the central region. Second, there is a marked flattening of the strong central field distribution into a disk-shaped form.

The illustrations presented here serve to indicate a considerable variability of field distributions arising from different charges on the z-axis. We do not know the actual charge distribution resulting from atmospheric discharges of more complex forms than the assumed simple model in Figure 2 except that the parametric conversion of magnetic energy distribution to electric energy is expected to be more complex, involving perhaps stability considerations of the final electrical system.

As discussed earlier, the ionized region with its emission of visible light is expected to coincide with the specific field pattern, and so is the shape of the observed light phenomenon. Power loss caused by light emission and thermal heating give rise to a gradual decline of stored energy. With the passage of time, the intensity is expected to gradually decay according to Equation 44, causing a corresponding shrinking of the ionization boundary and the overall ionized region. Finally, the electric field is expected to shrink below sustained ionization everywhere, at which time the glowing light phenomenon would disappear.

4. Expected Motion of Localized Field Concentrations of Ionized Regions

Observations of ball lightning and higher altitude light phenomena are invariably registered as lightning objects of some geometrical shapes, moving

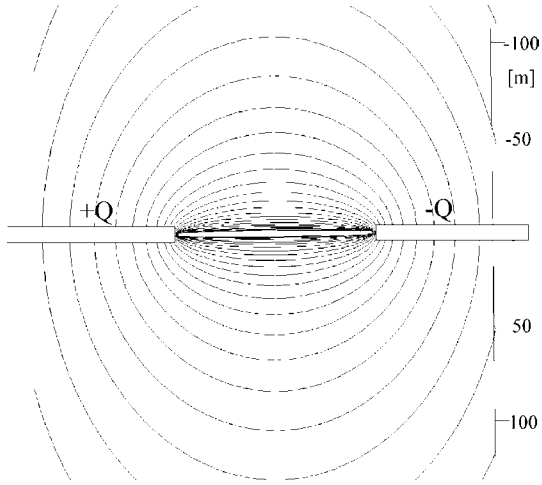

Fig. 9. Expanded view of the central region of Figure 8 showing the cigar-shaped field line configuration.

with more or less random acceleration, velocity and direction. How can this behavior be reconciled with the present concept of a spherical or near spherical circuit in free space with a localized region of ionized gas molecules? The explanation to this apparent puzzle might be tied in with the circumstance that the circuit is a separate electromagnetic entity whose localization in space is entirely independent of the ionized gas molecules, which merely serve as a small perturbation on the basic circuit. Therefore, its motion is expected to be determined by the environmental stray fields rather than by the ionized gas. No material ponderous forces are involved, only electric ones, causing the circuit itself to move in space. But what happens to the ionized region when the circuit itself is moving, leaving ionized gas molecules behind? The gas reacts by rapid deionization, whereas fresh gas molecules in front enter the high field region and become ionized, so that the overall shape remains the same, retaining an apparent stationary relation to the circuit, thereby creating the impression of a moving ionized region, whereas in fact the circuit with its strong field is the only thing moving. If we accept this explanation, the expected motion is a matter of interaction between the circuit and the environmental fields alone.

During thunder storms and also under less extreme atmospheric conditions there is often an abundance of charged clouds creating electric fields to ground or between clouds. A typical example is depicted schematically in Figure 11 showing a set of field lines between two oppositely charged clouds. The field distribution in the figure is sufficiently general to allow certain conclusions to be drawn concerning details of the interaction and motion. Although the environmental electric field might vary slowly with time due to variation of the charges in the clouds, or due to cloud motion, we shall assume that the field

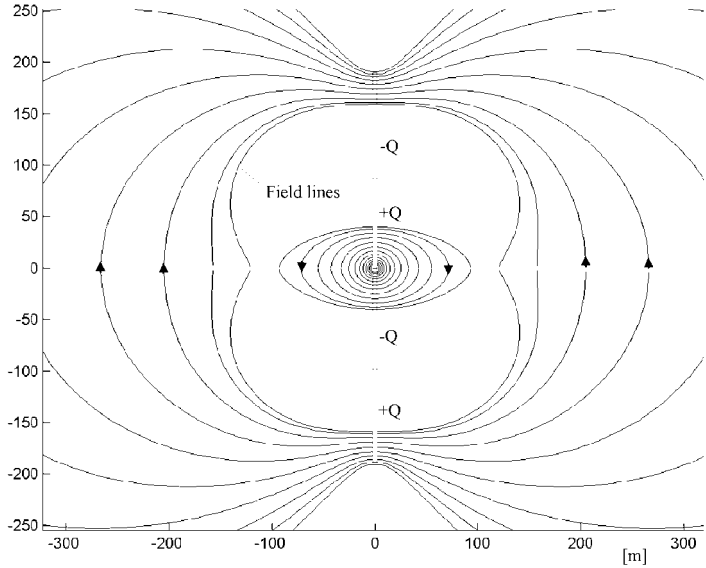

Fig. 10. Major perturbation of electric field distribution arising from a semiperiodic charge variation on the discharge axis, giving rise to a disk-shaped central region.

is stationary, and from there determine the expected motion of the ionized circuit exposed to the environmental field.

It is convenient to specify the presumably rotationally symmetric environmental electric field $\vec{\varepsilon}$ in a separate *cylindrical* coordinate system (ρ, z) with its z-axis coincident with the symmetry axis of the field, and with $\rho = 0$ and $z = 0$ representing the central symmetry point, as shown in the figure. Because of θ-independence, the field is specified by

$$\vec{\varepsilon}(\rho, z) = \varepsilon_z(\rho, z)\vec{a}_z + \varepsilon_\rho(\rho, z)\vec{a}_\rho \tag{57}$$

The lowest order approximations of the components $\varepsilon_z(\rho, z)$ and $\varepsilon_\rho(\rho, z)$ are given by:

$$\varepsilon_z(\rho, z) = \varepsilon_z(\rho) = -\varepsilon_{z0} + \varepsilon_{z2}\rho^2 \qquad \varepsilon_r(\rho, z) = 2\varepsilon_{z2}\rho z \tag{58}$$

where ε_{z0} and ε_{z2} are both positive, with the parameter ε_{z2} specifying the nonuniformity of the field. It is assumed that the original excitation of the ionized region was caused by the same charged cloud configuration producing the environmental field of Figure 11, so that the two z-axes coincide.

The forces acting on the circuit have their roots in the interaction between the environmental field and the magnetic field $\hat{h}_\phi$ produced by the current due to the conductivity of the ionized region. Because we shall find that the overall results of the interaction depend on symmetry arguments, which are the same regardless of the ionized shape, it suffices to consider the basic spherical region for which the magnetic field at the surface $r = r_i$ is obtained from Equation 35:

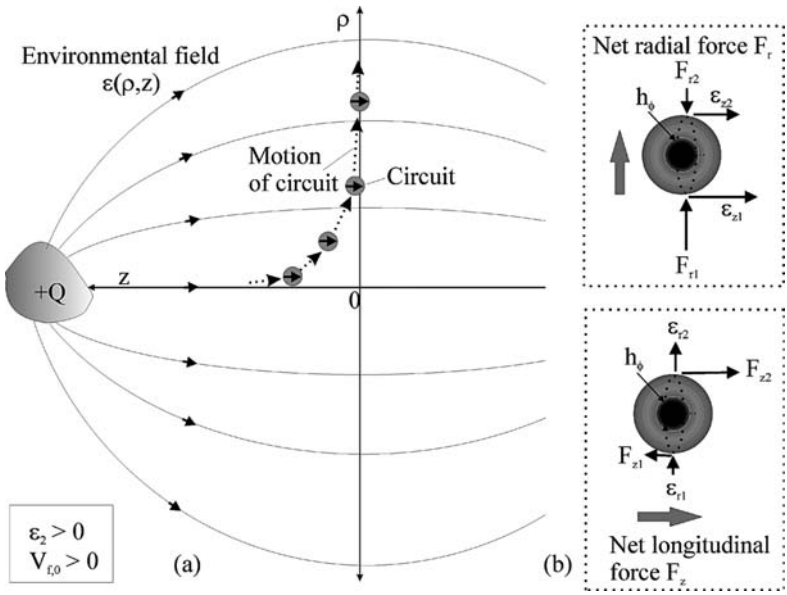

Fig. 11. (a) Expected motion of ionized circuit in the environmental field between two charged clouds in the case that the circuit and environmental field polarization are in the same direction: $V_{f,0}\varepsilon_2 > 0$. (b) Net radial and longitudinal force components at some displacement ρ_0, z_0 from the center.

$$r_i\vec{h}(r_i,\theta) = \vec{a}_\phi \frac{r\hat{\boldsymbol{h}}_\phi(r_i)}{\sin(\theta)} = -\vec{a}_\phi \frac{Z_0\sigma V_{f,0} r_i}{\sin(\theta)} \tag{59}$$

The force acting on the circuit is given by the net momentum divided by c, averaged over the surface S_c of the circuit.

$$\vec{F} = \frac{1}{cZ_0}\int\limits_{S_c}[\vec{e}(r,\theta)+\vec{\varepsilon}(\rho,z)]\times\vec{h}(r,\theta)]dS = \frac{1}{cZ_0}\int\limits_{S_c}[\vec{\varepsilon}(\rho,z)\times\vec{h}(r,\theta)]dS \tag{60}$$

Because the integral of $\vec{e}(r,\theta)\times\vec{h}(r,\theta)$ vanishes, the equation reduces to

$$\vec{F} = \frac{1}{cZ_0}\int\limits_{S_c}[\vec{\varepsilon}(\rho,z)\times\vec{h}(r,\theta)]dS \tag{61}$$

If the circuit is located at the symmetry point $\rho = z = 0$, the integral (Equation 61) vanishes due to symmetry, so that the force is zero. Let us investigate the stability by imaging the circuit center displaced to some point ρ_0, z_0 away from the zero point so that the circuit finds itself in a slightly non-uniform environmental field $\vec{\varepsilon}(\rho, z)$, in which case Equation 60 predicts non-vanishing force components obtained by substitution from Equations 57 and 59 into Equation 60.

$$F_\rho(\rho_0, z_0) = \vec{F}\cdot\vec{a}_\rho = \frac{\varepsilon_{z2}\sigma V_{f,0}}{c}\int_{S_c}(\vec{a}_z \times \vec{a}_\phi)\cdot\vec{a}_\rho \rho^2 \frac{dS}{\sin(\theta)} \tag{62}$$

$$F_z(\rho_0, z) = \vec{F}\cdot\vec{a}_z = -\frac{2\varepsilon_{z2}\sigma V_{f,0}}{c}\int_{S_c}(\vec{a}_z \times \vec{a}_\phi)\cdot\vec{a}_\rho z\rho \frac{dS}{\sin(\theta)} \tag{63}$$

Hence, the force components are proportional to averages over the sphere of ρ^2 and ρz, respectively. The averages are evaluated by expressing the variables in the integrand by the local circuit variables θ, ϕ.

$$\begin{aligned}(\vec{a}_z \times \vec{a}_\phi)\cdot\vec{a}_\rho &= \cos(\phi)\\ \rho &= \rho_0 + r_i \sin(\theta)\cos(\phi)\\ z &= z_0 + r_i\cos(\theta)\\ dS &= r_i^2 \sin(\theta)\cos(\phi)d\theta\, d\phi\end{aligned} \tag{64}$$

Substitution into Equations 62 and 63 and integration over θ and ϕ result in the following force components:

$$\begin{aligned}F_\rho &= F_\rho(V_{f,0}\varepsilon_{z2}\rho_0) = \frac{4\pi r_i^3}{c}\sigma V_{f,0}\varepsilon_{z2}\rho_0 \quad \text{[Newton]}\\ F_z &= F_z(V_{f,0}\varepsilon_{z2}z_0) = -\frac{4\pi r_i^3}{c}\sigma V_{f,0}\varepsilon_{z2}z_0 \quad \text{[Newton]}\end{aligned} \tag{65}$$

It is seen that the force components F_ρ and F_z are functions of the products $V_{f,0}\varepsilon_{z2}\rho_0$ and $V_{f,0}\varepsilon_{z2}z_0$, respectively, a fact simplifying the discussions of expected motions under various symmetry conditions. The various cases are illustrated in a set of Figures 11–13.

Case 1: $V_{f,0}\varepsilon_{z2} > 0$ *shown in Figure 11.* The direction of the environmental field is assumed to be coincident with the original discharge field, a likely condition but not necessarily always the case. Because the radial force F_ρ points in the direction of the radial displacement ρ_0, the symmetry axis $\rho_0 = 0$ does not represent a stable position. The smallest radial displacement gives rise to a force away from the axis. The axial force F_z is proportional to $-z_0$ and points towards $z = 0$ which therefore represents a stable position.

Under the stated circumstances the motion of the circuit with its ionized region is eventually taking place along the $z = 0$ plane, i.e., perpendicular to the z-axis, as shown in the figure. The preferred *direction* of motion in the $z = 0$ plane cannot be answered from the present rotationally symmetric model. In a more realistic non-symmetric model the motion is supposedly in the direction of the maximum field.

Case 2: $V_{f,0}\varepsilon_{z2} > 0$ *shown in Figure 12.* This case corresponds to a reversal of the environmental field ($\varepsilon_{z2} \to -\varepsilon_{z2}$) *or* reversal of the polarization of the circuit itself ($V_{f,0} \to -V_{f,0}$). Both force components F_ρ and F_z change direction, so that F_ρ is pointing towards the z-axis and F_z is pointing away from the symmetry point $z = 0$. As shown in the figure, the motion of the circuit is now

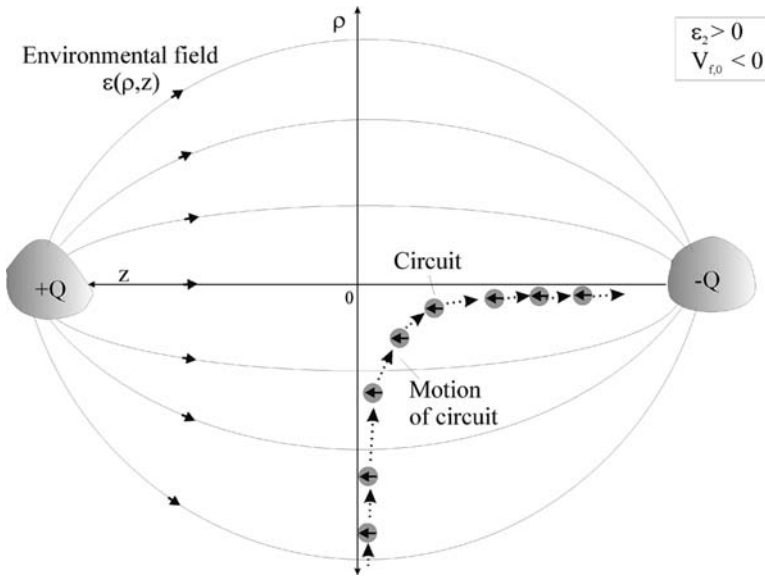

Fig. 12. Expected motion of ionized circuit in the environmental field between two charged clouds in the case that the circuit and environmental field polarization are in opposite direction: $V_{f,0}\varepsilon_2 < 0$.

taking place *along* the z-axis, in the positive or the negative direction, depending on the starting point.

Case 3: $V_{f,0}\varepsilon_{z2} < > 0$ *shown in Figure 13.* This is a more complex but still possible environmental field distribution in which the two conditions $V_{f,0}\ \varepsilon_{z2} > 0$ and $V_{f,0}\varepsilon_{z2} < 0$ apply in spatially separated regions of space, representing an approximate quadrupole field condition. The expected behavior follows directly from the previous cases indicated in Figures 11 and 12. The ionized object, presumably created at point A by a discharge between clouds A_+ and A_- first moves perpendicularly in the direction $A \rightarrow B$ until it reaches the radially stable but axially unstable point B, at which location its velocity is reduced instantaneously to zero, then turns abruptly 90 degrees and continues its motion in the direction $B \rightarrow C$ or possibly in direction $B \rightarrow C'$.

Hence, the quadrupole field environment might give rise to an abrupt-angle change of direction, i.e., infinite acceleration. From the simple examples discussed here it can be predicted that a more general environmental field configuration, produced by an aggregation of charged clouds, might possibly give rise to many different and random flight paths of the object, involving high speed and abrupt velocity and acceleration changes. What accelerations and velocities can be expected? Since no regular inertia effects are involved, the velocity $\vec{v}$ rather than acceleration $d\vec{v}/dt$ is expected to be *proportional* to the electromagnetic force $\vec{F}$ determined by the environmental field, so that $\vec{v} \sim \gamma F$,

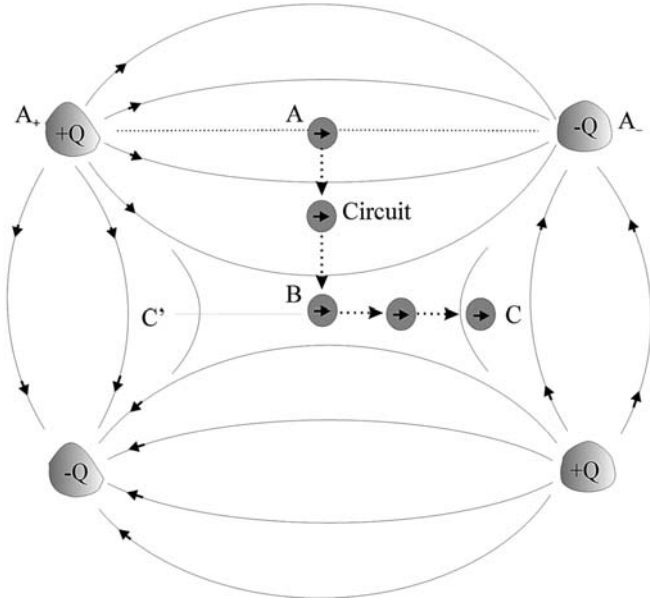

Fig. 13. Motion of ionized circuit in a quadrupole type environmental field, exhibiting abrupt angle directional change.

where the drag parameter γ represents the retarding force due to the inertia of the continuous front end ionization process of air taking place during the flight. Limited knowledge of the ionization processes and other parameters prevent any estimate of velocity ranges. What can be said with some certainty is that acceleration limitation is not an issue, since no ponderous forces are involved. In particular, the theory predicts the possibility of abrupt changes of direction, a dramatically different behavior from regular objects with mass.

5. The Ball Lightning Phenomenon

The described electromagnetic process, identifying the final state of ball lightning as a slowly decaying *DC* spherical standing wave of electric field, assumes a model of uniform free space environment with no disruptions of the symmetry of the overall transmission system. This idealized model can hardly be expected to hold in any practical ball lightning occurrence, which does not take place in an infinite space completely free of material and other environmental influences. Such effects are by their nature quite complex, and a general discussion is beyond the scope of the present paper. In view of the general discussion in Section 4, it is possible to understand a few typical patterns in ball lightning observations, which seem to be tied in with environmental perturbations to be discussed in the next sections. The first pattern is the observed

random, but predominantly horizontal, motion of the ball near ground. The second is the observation of lightning balls suddenly disappearing accompanied by a more or less violent explosion and release of energy.

5.1. Location and Motion of the Ball Lightning Sphere

Atmospheric discharges between charged clouds and ground take place in an asymmetric environment, with ground representing an imperfect plane of symmetry. The excited circuit is therefore asymmetric with its symmetry plane at or close to ground with charges in the ground replacing the lower part of the charged column along the z-axis.

The energy dissipation in the ionized region is expected to raise the temperature, causing a small expansion and reduced density, whereby its balance with the surrounding air is upset. At first glance, the precariously delicate balance of this so-called "hot balloon effect" between the ionized sphere and the surrounding air would cause the sphere to ascend rapidly towards higher altitudes. But this behavior is not reported as a typical characteristic of ball lightning. On the contrary, most observations indicate horizontal motion in a more or less random direction, and sometimes downward motion of the ball. How can the absence of upward motion be reconciled with localized heating of the ionized sphere? One perhaps rather unlikely explanation is that most of the energy is dissipated as emitted light, with only negligible heating. A more likely explanation was discussed earlier linking the absence to lack of electromagnetic coupling between the basic circuit field and the gas molecules in the ionized sphere. According to this picture the heated air is indeed moving upwards, out of the influence of the circuit's electric field, in the process losing its ionized state on the topside, with fresh cool air being continuously replaced and ionized on the bottom side.

The predominant horizontal motion of ball lightning is covered by the explanations offered in Section 4, notably by Figure 11. The asymmetric cloud to ground case appropriate to the ball lightning case is further illustrated in Figure 14. Whereas $z_0 = 0$ is a stable position, $\rho_0 = 0$ is not. Therefore, the ball moves horizontally with its localized fields and stored electromagnetic energy, while the air itself remains stationary with fresh air being ionized at the front end and air being deionized at the rear end. Thus, the motion of the ionized sphere is only apparent.

The commonly reported observations of *random* horizontal motion of ball lightning might be interpreted as attempts of the ball to position itself where the environmental vertical field is constant and independent of radius. At such positions the radial force vanishes so that the ball remains in a stationary position. In addition, localized electric fields arising from various electric disturbances and uneven ground geometry and conductivity are certainly expected to contribute to the complexity of the overall field pattern, and therefore to the random motion of the ball lightning.

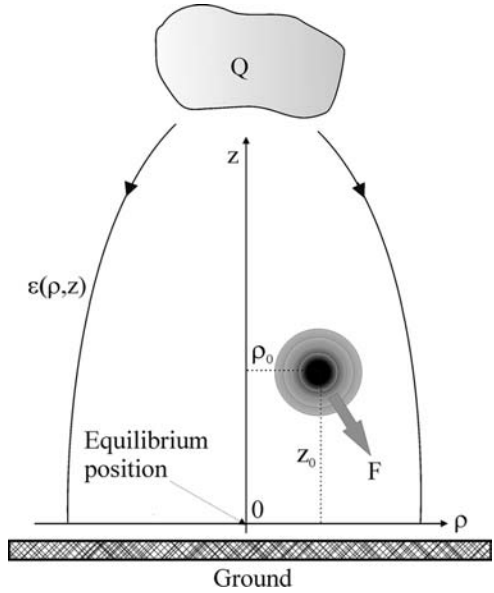

Fig. 14. Illustration of the environmental field of a positively charged cloud and the force F acting on the ball lightning sphere at some small displacement ρ_0, z_0 from the center.

The many mysterious observations of ball lightning moving *through* walls and window panes (Grigor'ev et al., 1992) have a similar explanation and are readily understood because non-conducting dielectric materials with dielectric constants different from free space represent no hindrances for the circuit fields. The circuit just leaves the ionized ball behind in deionized and invisible condition and ionizes a similar ball on the other side. The penetration of the ball is only apparent. Damage to walls and windows, sometimes even including melting, are explained by losses in the dielectrics and high electric field concentration at the point of penetration.

5.2. Violent Explosion of Ball Lightning

Observations and reports of violent ball lightning explosions might be tied in with environmental perturbations of a different kind. With reference to Figure 7, the z-axis of the spherical transmission line contains charges $+Q$ and $-Q$ serving to terminate the electric field lines e_θ over the entire length L of the spherical transmission line. The ball lightning occurs near conducting ground, serving as a somewhat irregular symmetry plane, with appropriate ground charges replacing the lower charge column in Figure 7. Random objects on the ground are bound to upset the symmetry in various ways, thereby affecting the behavior of the ball. Because the ionized ball itself is presumably a neutral plasma it is expected to be quite insensitive to encounters with metallic objects, as indeed

verified by numerous observations. But the situation might be different if the ball touches the conducting object with the above ground charged column, giving rise to a major catastrophic event in which all or part of the column might discharge into the metallic object, upsetting the overall symmetry of the electric field. Recalling that the electric field varies as $1/r$, it might be expected that such a symmetry upset has dire consequences for the stability of the ionized sphere. Even if we are unable to be more specific about possible environmental perturbations that might cause such stability disruptions, we are able to describe the expected *response* on the field distribution of the spherical transmission line. From an electromagnetic point of view the symmetry upset gives rise to a corresponding modification of the local field pattern near $r = 0$ and therefore a change of the terminating impedance at the input end, and such load impedance changes are readily handled from regular transmission line theory, as demonstrated in the following.

With reference to the illustrations in Figure 4, the distributed termination susceptance at the input end represent an open circuit, thus providing complete reflection of the inward wave $V_b(r + T)$ into $-V_f(r - T)$ resulting in the electric standing wave described in the earlier sections. The condition of perfect reflection is contingent upon perfect symmetry of the charged column above ground and the equivalent charges in the ground. With the assumed disruption of symmetry the terminating impedance is reduced from infinite to some finite value, thereby upsetting the balance of the *DC* standing wave along the line. The new impedance depends on the nature of the perturbation, but regardless of details, the response of the line exhibits some typical characteristics. A good idea of the expected response is gained by considering a reduction of the terminating impedance from infinite to a resistive load equal to the characteristic impedance Z_w of the transmission line.

The abrupt change of terminating load calls for a corresponding excitation of extra pulses of the same type as the pulses $V_f(r - T)$ and $V_b(r + T)$ constituting the original stable *DC* distribution illustrated in Figures 4c and 5. The process is identical to a sudden discharge of a transmission line through a resistor, a familiar example in textbooks on transmission circuits. The sketches in Figure 15 illustrate how this simple process develops as a function of time from the original unperturbed state at time $T = 0$, shown in Figure 15a. The sudden reduction of load impedance to Z_w calls for the excitation of an extra outward pulse $V_f(r - T)'$ of opposite sign to the original $-V_f(r - T)$. During the normalized time interval $0 < T < r_{\max}$, the situation corresponds to Figure 15b showing the progressive canceling of the overall outward wave components. At the end of this interval the canceling is complete so that the inward component $+V_b(r+T)$ fails to be excited at $r_{\max}$ by reflection of the original $-V_f(r-T)$. The necessary compensation takes place through excitation of a second inward pulse $-V_b(r+T)'$ of opposite sign, as shown in Figure 15c, which shows the situation in the interval $r_{\max} < T < 2r_{\max}$. At the end of the full round trip of duration $t = T/c = 2r_{\max}/c$ the electric field has been reduced to zero along the entire line. During this

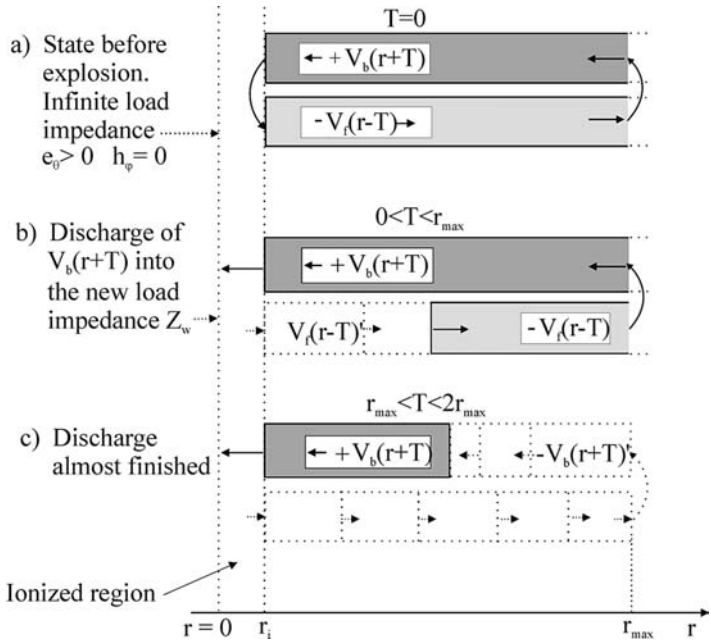

Fig. 15. Illustration of a sudden discharge due to some unspecified major perturbation. (a) Unperturbed state. (b) The state immediately after a catastrophic reduction of load impedance, causing excitation of a forward pulse $V_f(r-T)$ of opposite sign, successively reducing the electric field to zero along the line. (c) The state immediately before the line is fully discharged. After a time expenditure of $\Delta t = 2r_{\max}/c$, the full energy has been discharged into the new load impedance, resulting in a violent explosion.

short time interval the stored electrical energy is continuously discharged into the localized load representing the perturbed region of the ionized sphere, in the form of a transient pulse of energy. The sudden release of a large amount of stored energy must appear as a violent explosion of the lightning ball with a release of all its energy, after which it ceases to exist.

The sequence of events illustrated in Figure 15 refers to a load equal to the characteristic impedance Z_w of the spherical transmission line, in which case the energy discharge is complete after just one roundtrip of duration $t = 2r_{\max}/c$. The case of a general load impedance is a little more complex in that a few roundtrips of successively smaller pulse amplitudes are required to fully discharge the line, but the expected final result is invariably the same violent explosion.

5.3. Summary of Ball Lightning

The theory describes the ball lightning phenomenon as the end state of an electromagnetic process originating with the accumulation of electric charges in thunderclouds with the buildup of static electric energy in the space between

the cloud and ground. Triggered by the thunderbolt itself, the subsequent development initiates a complex process in which the electric energy, less a small radiation and dissipation loss, is converted to predominantly magnetic energy driven by the current in the discharge column. At the sudden termination of the current the magnetic energy cannot be sustained any more, and is converted back to electric energy in an electromagnetic transient process compatible with Maxwell's equations, leading to the special solutions described in the paper.

According to this picture the ball lightning phenomena are aftermaths of the thunderbolt itself, with electric energy comparable to the original electric energy minus the radiation and dissipation losses, just appearing in a different and highly localized form, characterized by a highly localized field, rather than the original fields of the clouds. Even if such conversions may happen on a regular basis there does not seem to be any guarantee that the conversion process results in the formation of lightning objects such as ball lightning, which is known to be a relatively rare occurrence. A possible explanation for the rarity might be tied in with additional requirements and preconditions such as shape and distribution of the strike itself, minimum energy demands, and various unspecified environmental constraints.

5.4. Comparison With Typical Observations

In the following we shall discuss how well the proposed theory explains reported qualitative features of typical and characteristic observations of ball lightning phenomena.

The theory explains the many reports that the balls are directly created by a lightning bolt, as well as its tendency to remain close to ground with predominantly horizontal motion. Speed and motion are determined entirely by the electromagnetics of the circuit and its interaction with environmental fields, not by the air, which just happens to be ionized by the strong fields at the center. The equilibrium position near ground also explains observations of balls falling at high speed from the upper atmosphere and stopping before hitting the ground. In particular, the motion of the ionized ball of air is only apparent. Hence, there are few restraints on the motion characteristics other than those arising from the electromagnetic properties of the material substances that happen to constitute the environment.

The absence of direct coupling between the strong electric field of the circuit and the sphere of ionized air explains a number of observations such as motion independence of wind or turbulence, absence of ''the hot balloon effect,'' and penetration through window panes and walls.

Wind and turbulence are expected to sweep away the ionized air from the high field center of the electromagnetic circuit, but new entering air molecules are continuously ionized, creating the appearance that the lightning ball remains stationary, quite independent of wind.

The same process also explains the ''hot balloon effect.'' The heated air in the ball is expected to move upwards because of the very precarious balance

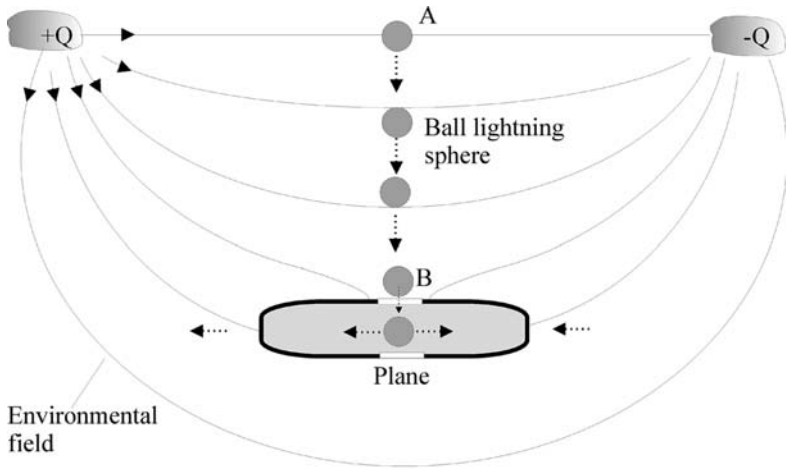

Fig. 16. Illustration of a ball lightning sphere attracted to a plane via the perturbed environmental field at the plane, and a possible penetration into the plane through a side window.

between hot and cold air. In this process the upward moving air is deionized and replaced with new air, which is continuously ionized so that the lightning ball remains in the same stationary position.

Penetration through windows and non-conducting walls is explained similarly. What moves through the material walls is just the high field circuit, leaving the ball behind in deionized condition and ionizing a similar ball on the other side. Reported observations of damage to windows, sometimes even melting of holes, are supposedly caused by localized heat generation at the point of penetration due to high field and glossy windowpanes.

Reports of ball lightning observed inside airplanes (Grigor'ev et al., 1992) are special in the sense that they happen well above ground in a relatively small closed space almost completely surrounded by the metallic aircraft body forming an almost perfect Faraday cage. Because it is unlikely that the ball lightning originates inside the aircraft itself, it must enter from the outside. The windshield in modern aircrafts is a composite sandwich of materials with a coated layer of surface conducting material. Therefore, penetration through the windshield is unlikely, whereas the normally uncoated side windows might be possible points of entry. Since this phenomenon takes place at great heights rather than close to ground, it is probably due to the aftermath of an *intracloud* discharge (see Figure 1) rather than a cloud to ground discharge. Although the initial formation of the ball happens away from the plane, the subsequent motion in the environmental field might carry the ball towards the plane. Figure 16 illustrates a possible situation in which the plane finds itself in a position relative to the charged clouds that environmental field lines terminate on the plane's conducting body. The ball is originally excited at point *A* half way between the

charged clouds. According to the general discussion in connection with Figure 11 the subsequent motion of the ball is taking place along the direction $A \rightarrow B$, i.e., towards the plane. The field lines form a stability region for the ball at or near the plane. Hence, if conditions are right, outside ball lightnings caused by intracloud strikes might be attracted to planes. Because the local environmental field at the plane moves with the speed of the plane, the ball moves with it, maintaining its position at the stability point. As we have seen there is no immediate limit to speed.

But why is the ball moving through the window? The outside metallic body of the aircraft represents an approximate symmetry plane for the electric field lines e_θ of the overall spherical circuit. Not normally excited, a similar spherical circuit exists inside the aircraft, although it must be strongly perturbed by the metallic enclosure. However, this is not expected to materially affect the spherical field distribution near $r = 0$ presumably located at the window. The inside and outside spherical circuits are presumably coupled together through the non-conducting windowpane. The two circuits might represent a bistable system with preference of either the external or the internal circuit excited, depending on geometrical details and environmental field distributions. If the internal circuit is the preferred one, with penetration through a side window and formation of ball lightning inside the plane, the subsequent motion of the ball inside the aircraft is expected to be determined by the local internal environmental fields.

Reported observations of ball lightning emitting a hissing sound might be understood from the discussion in Section 3.3 for the case of a striking bolt to ground from large height L and high energy. In such cases the *RF* electromagnetic oscillations superimposed on the basic *DC* circuit field are fairly low frequency, possibly exciting audible acoustic vibrations through non-linear coupling effects.

Observed violent explosions of the ball might be explained from a random disruption of the basic circuit symmetry. The ionized air in the ball is considered a charge neutral plasma. The absence of net charge is in agreement with observations that the ball does not normally discharge when touching a conductor. Minor attraction to conductors and motion along metallic fences may be due to the charges in the z-axis column. Normally the column is supposed to be stable and not expected to discharge. However, the discussion in Section 4.1 describes a scenario in which the symmetry of the charge column might be sufficiently disrupted by some unspecified environmental effects to cause collapse of the otherwise balanced electromagnetic circuit. With the assumption that the lightning ball can indeed be exposed to such large disruptions and subsequent symmetry collapse, all the energy stored in the spherical transmission line is subsequently discharged as a transient pulse of very short duration, a phenomenon that must have the appearance of a violent explosion and disappearance of the lightning ball.

Comparison of observed lifetimes with the theoretical discussion in Section 3.2 is hampered by insufficient knowledge of the details of the ionization

process and dissipation mechanisms, and the paper does not claim to have anything close to a complete solution of this problem. The theory uses a simple model of current flow based on a macroscopic conductivity parameter σ for the entire ball, but estimates of σ under the extreme conditions of excessive and non-uniform electric field strength, including possible non-linearities and saturation phenomena, are extremely difficult. Therefore, dissipation and lifetime are subject to the same uncertainty. On the other hand, the dissipation is a perturbation parameter completely disconnected from the electromagnetic processes relating to the spherical transmission line constituting the basic circuit of the lightning ball. These processes are claimed to be the primary cause of the ball lightning phenomenon, with accurate knowledge of the amount of dissipation playing a secondary role. Similarly, the question of colors and luminosity of the emitted light from the ionized air is not addressed. But it appears probable that the large variation of electric field strength within the sphere must affect the relative ionization of the various types of air molecules, thereby accounting for the variety of colors in the observations.

In summing up the discussion, the bulk of typical observations appear to be compatible with the theoretical predictions offered in the paper, with no obvious contradictions to be noticed. Since the proposed theory satisfies the basic criteria of compatibility that any theory must pass, it comes forward as a strong candidate for explaining the ball lightning mystery. However, the theory does not claim to offer a complete understanding of all aspects and details of ball lightning. In particular, we need a better understanding of the details of the parametric excitation process, and the ionization, dissipation, and light emission phenomena under high intensity electric fields.

6. Higher Altitude Light Phenomena

There exists a tremendous number of observations of higher altitude light phenomena, ranging from sightings classified as Unidentified Flying Objects (UFOs) to more mundane sightings of light occurrences of various shapes, such as those seen on a more or less regular basis in Hessdalen (Sturrock, 1999: 78–80). Although a comprehensive analysis of such events is way beyond the scope of the paper, we shall discuss whether typical characteristics of light emitting objects in the sky can be fitted into the presented ball lightning theory. In particular, can the excitation of generally larger object sizes with longer lifetime, a multitude of different shapes, and the apparent speed and acceleration mystery be explained?

From the data presented in Section 3.3 the size is directly related to the stored energy. Therefore, large size means large energy. Accepting the formula (Equation 55) as a guide, a lightning object of 10 meters diameter excited by a discharge string of 1000 meters contains approximately 0.5×10^9 joule. Since this energy is in the range of energies in a typical lightning discharge (Uman, 1987), the existence of large objects is not out of the question. Observations of

long lifetime are difficult to explain from Equation 43 unless the conductivity σ is very small. Not very much is known about this parameter except that it is the macroscopic representation of collisions between electrons and gas molecules in accordance with Equation 26. In principle, the collision energy could be transferred to mechanical energy in the form of heat, or to molecular excitations accompanied by energy loss in the form of light emissions. Since energy loss in the form of heat is a volume effect proportional to r_i^3, i.e., to stored energy W, whereas loss through light emission might be proportional to the surface area r_i^2, i.e., to $W^{2/3}$, it can be speculated that a dominance of the latter will result in slower decay. This fairly speculative explanation would explain the observations of longer lifetimes.

Besides having generally large sizes and energies, the multitude of different shapes appears to distinguish the higher altitude sightings from the usual spherical shape of ball lightning. A discharge pattern more complex than the linear discharge model of Figure 5 might give rise to modifications of the spherical shape, as illustrated in the simple examples presented in Figures 7 through 10 in Section 3.4. All of these shapes are results of various modifications of the charge distribution on the z-axis of the excited circuit associated with a more complex discharge column. The most notable ones are Figures 9 and 10 showing disk-shaped and cigar-shaped ionized regions, typical forms of many UFO sightings and reports. Even more complex discharges and charge distributions than the ones illustrated in these figures might possibly give rise to a variety of different object shapes.

The theoretical explanation of the motion of ionized circuits subject to environmental electric fields originating in charged clouds, discussed thoroughly in Section 4, applies equally well to ball lightning and to higher altitude lightning objects. According to the presented theory, the preferred directions of motions are determined solely from symmetry relations of the environmental field. In particular, since no ponderous forces are involved, there are no immediate limits on acceleration, so that abrupt changes of direction are permitted.

Rather than undertaking a comprehensive discussion of possible motion characteristics, we shall dwell with just one typical sighting described in great detail in Sturrock (1999: 299–372), and show that several typical observations of this event are compatible with the present theory. The observations were made by the crew on a regular helicopter flight flying on a northerly course. The following is a very brief account of the essential observations. A cigar-shaped object, seen at some distance to the east, was observed to close in on the craft with speed estimated to 600 knots, decelerating and hesitating for a moment, then making a complete stop at close range to match the speed of the helicopter, then hovering in front and above the helicopter for some time estimated to be a few minutes, after which it rapidly took off in a westerly direction and disappeared beyond the horizon. During the encounter the object was emitting strong lights of red, white, and green colors. A magnetic compass was observed

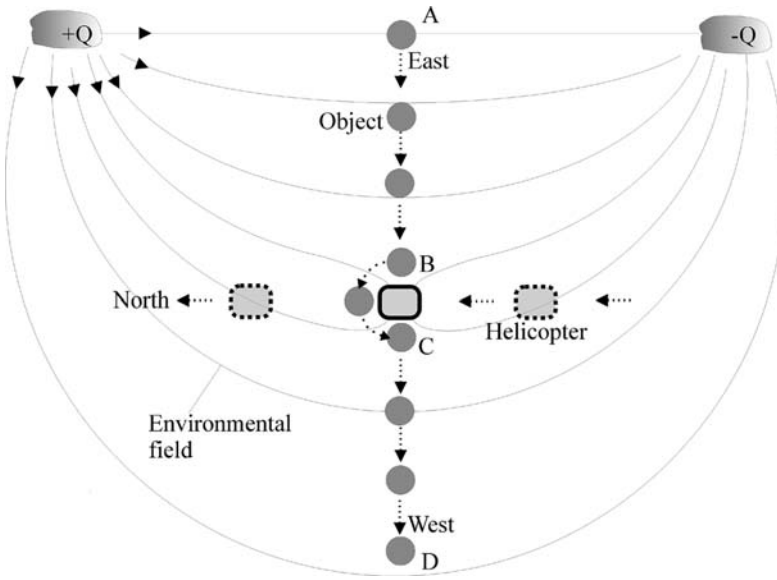

Fig. 17. Illustration of the encounter discussed in the text. The object, originating at point A moves along the path $A \rightarrow B$ directed by the symmetry of the environmental field from the charged clouds. It is temporarily anchored in a local stability region near the helicopter, then continuing on its original westward course $C \rightarrow D$.

to behave irregularly in that the magnetic needle was observed to turn at some fairly slow rate indicating the presence of strong magnetic fields.

We shall attempt to explain the observations, tentatively identifying the object as a localized region of ionized gas of the kind discussed in the paper. We shall assume a hypothetical scenario illustrated schematically in Figure 17, showing the helicopter subject to environmental fields originating from an aggregation of charged clouds. We have no way of knowing whether this cloud formation was in fact the actual cloud system at the time, but it certainly is a possible configuration which is selected because it fits the observations fairly well. The helicopter is part of the general environment, providing a local perturbation of the environmental field, forcing the field lines to be perpendicular to the metallic body.

It is assumed that the ionized object is excited through an intracloud discharge in accordance with the present theory, with initial location at point A in the figure. The environmental electric field shown in the figure is presumably caused by remnant charges in the same clouds. With reference to the discussion in Section 4, in particular Figure 11, the initial location A is not a stable one. With the shown relative orientation of clouds and helicopter, the object is subject to a force in direction $A \rightarrow B$, i.e., towards the helicopter. The force is a consequence of non-uniformity in the field, which is likely to be modified at or near the helicopter metallic walls, with possible local regions of field uniformity

where the object, anchored in a local stability region, is expected to suddenly decelerate and stop. Because the local fields are moving along with the aircraft, the object is also moving with the same speed as the aircraft. Because the local environmental field near the metallic helicopter body might be changing slowly due to the motion of the craft relative to the clouds, it is expected that the object, in seeking to remain in a stability region, adjusts its position relative to the helicopter correspondingly. The westerly take off along the direction $C \rightarrow D$ is interpreted as a continuation of the approach flight along $A \rightarrow B$. In this interpretation the object's stable and normal flight path would have been an uninterrupted course along $A \rightarrow D$, which is merely interrupted by the helicopter's perturbation of the environmental fields, causing a temporary stop of the object's normal flight.

The emission of white, red, and green light from different parts of the object might just relate to the presumably large range of electric field strength over the object's body, with expected differences in the ionization of constituent gas molecules.

During the encounter the helicopter is supposedly exposed to the strong electric and magnetic fields from the object. Whereas the electric field does not penetrate the metallic body, the magnetic field does, thereby affecting field-sensitive instruments such as the magnetic compass, which was showing irregular behavior. The details of field exposure can be estimated from the discussion in Section 3, where the *DC* magnetic field outside the ionized region was specified by

$$\vec{h}(r,\phi)_{\phi} \sim \frac{1}{r}\vec{a}_{\phi} = \frac{1}{r}\left[\vec{a}_x \cos(\phi) - \vec{a}_y \sin(\phi)\right] \tag{66}$$

When the object is at close range and its position relative to the helicopter is changing, the equatorial angle ϕ observed from inside the helicopter at the position x, y of the compass varies accordingly, with a corresponding continuous variation of the magnetic field. With the object fairly close to the helicopter, r is moderate, and the magnetic field might not be negligible compared to the earth's magnetic field. Under such circumstances the magnetic compass needle must point in the direction of the imposed field rather than the earth's magnetic field, in accordance with actual observations by the crew. This is significant evidence that the fields of the lightning object are of the *DC* kind discussed in the paper, not high frequency. If high frequencies were involved, the magnetic needle would not be able to overcome its inertia to follow magnetic field variations.

In view of the observations that the object's flight trajectories include abrupt angle turns and speeds ranging from zero to some 600 knots, these characteristics disqualify it as a natural phenomenon of solid objects with mass. The same limitations on acceleration and speed do not apply to ionized regions of the type presented in the paper, which therefore fit reasonably well the observations, with no obvious contradictions.

In summary, the question posed at the beginning of this section, whether

typical characteristics of light emitting objects in the sky can be fitted into the presented ball lightning theory, must be answered in the affirmative. The linking of seemingly quite different sightings to a common origin provides a platform from which we might hope to dig further into the tremendous complexity and enigma of these natural phenomena.

References

Endean, V. G. (1976). Ball lightning as electromagnetic radiation. *Nature, 263,* 753.

Grigor'ev, A. I., Grigor'eva, I. D., & Shiryaeva, S. O. (1992). Ball lightning penetration into closed rooms: 43 eyewitness accounts. *Journal of Scientific Exploration, 6*(3), 261–279.

Jackson, J. D. (1975). *Classical Electrodynamics.* Wiley.

Kapitza, P. L. (1958). Uber die Natur des Kugelblitzes. *Physikalische Blatter, 14,* 11.

Stenhoff, M. (1999). *Ball Lightning—An Unsolved Problem in Atmospheric Physics.* Plenum Press.

Sturrock, P. A. (1999). *The UFO Enigma.* Warner Books.

Uman, M. A. (1987). *The Lightning Discharge.* Academic Press.

Wessel-Berg, T. (2000). *Electromagnetic and Quantum Measurements: A Neoclassical Bitemporal Theory.* Kluwer Academic.

Wessel-Berg, T. (2003). A proposed theory of the phenomenon of ball lightning. *Elsevier, Physica D, 182,* 223–253.